Cell

A natural gene drive system confers reproductive isolation in rice

Graphical abstract

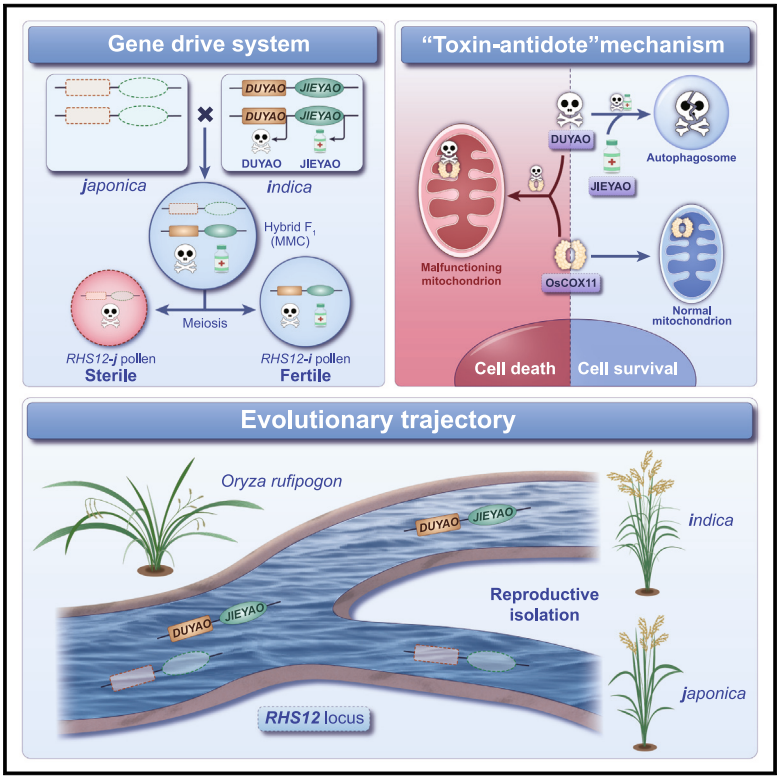

Highlights

- *DUYAO-JIEYAO* encodes a toxin-antidote system that confers hybrid male sterility
- DUYAO interacts with OsCOX11 to trigger mitochondrial malfunction and cytotoxicity
- JIEYAO detoxifies DUYAO by rerouting DUYAO to the autophagosome for degradation
- *DUYAO-JIEYAO* forms a natural gene drive system that may promote speciation in rice

Authors

Chaolong Wang, Jian Wang, Jiayu Lu, ..., Haiyang Wang, Chuanyin Wu, Jianmin Wan

Correspondence

wanghaiyang@caas.cn (H.W.), wuchuanyin@caas.cn (C.W.), wanjianmin@caas.cn (J.W.)

In brief

A cytotoxicity-detoxification gene drive system entailing mitochondria-autophagosome interaction confers hybrid male sterility in rice.

Wang et al., 2023, Cell *186*, 3577–3592
August 17, 2023
https://doi.org/10.1016/j.cell.2023.06.023

CellPress

Cell

CellPress
OPEN ACCESS

Article

A natural gene drive system confers reproductive isolation in rice

Chaolong Wang,[1,2,8] Jian Wang,[2,8] Jiayu Lu,[1,8] Yehui Xiong,[2,3,8] Zhigang Zhao,[1] Xiaowen Yu,[1] Xiaoming Zheng,[2] Jing Li,[4] Qibing Lin,[2] Yulong Ren,[2] Yang Hu,[1] Xiaodong He,[1] Chao Li,[1] Yonglun Zeng,[5] Rong Miao,[1] Mali Guo,[6] Bosen Zhang,[7] Ying Zhu,[5] Yunhui Zhang,[1] Weijie Tang,[1] Yunlong Wang,[1] Benyuan Hao,[1] Qiming Wang,[1] Siqi Cheng,[1] Xiaojuan He,[1] Bowen Yao,[1] Junwen Gao,[1] Xufei Zhu,[1] Hao Yu,[1] Yong Wang,[1] Yan Sun,[1] Chunlei Zhou,[1] Hui Dong,[1] Xiaoding Ma,[2] Xiuping Guo,[2] Xi Liu,[1] Yunlu Tian,[1] Shijia Liu,[1] Chunming Wang,[1] Zhijun Cheng,[2] Ling Jiang,[1] Jiawu Zhou,[4] Huishan Guo,[7] Liwen Jiang,[5] Dayun Tao,[4] Jijie Chai,[3] Wei Zhang,[6] Haiyang Wang,[2,*] Chuanyin Wu,[2,*] and Jianmin Wan[1,2,9,*]

[1]State Key Laboratory of Crop Genetics & Germplasm Enhancement and Utilization, Nanjing Agricultural University, Nanjing 210095, China
[2]State Key Laboratory of Crop Gene Resources and Breeding, Institute of Crop Sciences, Chinese Academy of Agricultural Sciences, Beijing 100081, China
[3]Beijing Advanced Innovation Center for Structural Biology, Tsinghua-Peking Joint Center for Life Sciences, School of Life Sciences, Tsinghua University, Beijing 100084, China
[4]Food Crops Research Institute, Yunnan Academy of Agricultural Sciences, Kunming 650200, China
[5]Centre for Cell & Developmental Biology and State Key Laboratory of Agrobiotechnology, School of Life Sciences, The Chinese University of Hong Kong, Shatin, New Territories, Hong Kong, China
[6]College of Animal Science and Technology, Nanjing Agricultural University, Nanjing 210095, China
[7]State Key Laboratory of Plant Genomics, Institute of Microbiology, Chinese Academy of Sciences, Beijing 100101, China
[8]These authors contributed equally
[9]Lead contact
*Correspondence: wanghaiyang@caas.cn (H.W.), wuchuanyin@caas.cn (C.W.), wanjianmin@caas.cn (J.W.)
https://doi.org/10.1016/j.cell.2023.06.023

SUMMARY

Hybrid sterility restricts the utilization of superior heterosis of *indica-japonica* inter-subspecific hybrids. In this study, we report the identification of *RHS12*, a major locus controlling male gamete sterility in *indica-japonica* hybrid rice. We show that *RHS12* consists of two genes (*iORF3/DUYAO* and *iORF4/JIEYAO*) that confer preferential transmission of the *RHS12-i* type male gamete into the progeny, thereby forming a natural gene drive. *DUYAO* encodes a mitochondrion-targeted protein that interacts with OsCOX11 to trigger cytotoxicity and cell death, whereas *JIEYAO* encodes a protein that reroutes DUYAO to the autophagosome for degradation via direct physical interaction, thereby detoxifying DUYAO. Evolutionary trajectory analysis reveals that this system likely formed *de novo* in the AA genome *Oryza* clade and contributed to reproductive isolation (RI) between different lineages of rice. Our combined results provide mechanistic insights into the genetic basis of RI as well as insights for strategic designs of hybrid rice breeding.

INTRODUCTION

Reproductive isolation (RI) is a universal biological phenomenon that restricts gene flow between populations and thus serves as both an indicator of speciation and a mechanism for maintaining species identity. Multiple pre-fertilization (pre-zygotic) and post-fertilization (post-zygotic) barriers, such as niche differentiation, phenological isolation, and various forms of hybrid incompatibility (HI), could contribute to RI in animals and plants.[1–4] HI refers to deleterious hybrid characteristics that result in intrinsically reduced fitness of the inter-specific or inter-population hybrids (such as hybrid sterility [HS], necrosis, and lethality etc.), which thereby promote RI between diverging populations.[5]

The genomic conflict hypothesis posits that conflict between different parts of the genome acts as a driver of HI.[6,7] In particular, recent studies have identified a class of selfish genetic elements variously called toxin-antidote elements/meiotic drives/gene drives that underlie genetic incompatibility between different wild populations in the plant and animal kingdoms. They ensure their biased transmission to the progeny by killing the non-carriers and thus subverting Mendel's law of segregation.[1,8–10] Although such elements usually consist of two or three tightly linked factors, they share no homology among fungi, plants, and animals, and their underlying molecular mechanisms remain poorly resolved.[11–18]

HS is the most common form of HI and a major limiting factor hampering utilization of the strong heterosis between the *indica-japonica* subspecies or between cultivated and wild rice for crop breeding.[19] Dozens of genetic loci controlling HS have been identified in rice[20,21]; and among them, 12 HS loci have been cloned, including *S1*, *Sa*, *Sc*, *qHMS7*, and *S5*.[22–27] Notably, several of these have been shown to form "toxin-antidote" or

"killer-protector" systems.[8,9,20] For example, the *S5* locus, controlling embryo sac fertility in the F_1 hybrids of *indica* and *japonica* subspecies, is composed of three *ORFs*; *ORF5+* (encoding a killer), *ORF4+* (encoding a partner), and *ORF3+* (encoding a protector). During female sporogenesis, *ORF5+* and *ORF4+* work together to induce endoplasmic reticulum stress, resulting in programmed cell death and leading to abortion of the embryo sac carrying *ORF3−*. However, the gametes carrying *ORF3+* can develop normally and are preferentially transmitted to the next generation.[26] The *qHMS7* locus controlling pollen sterility in the F_1 hybrid of Asian cultivated rice with *O. meridionalis* is composed of *ORF2* (encoding a toxin) and *ORF3* (encoding an antidote). In the process of male gametogenesis, *ORF2* aborts pollen grains in a sporophytic manner, whereas the mitochondrion-localized ORF3 protects pollen grains in a gametophytic manner, thereby leading to selective transmission of the *ORF3*-carrying pollen grains to the progeny.[27] Despite the major progress made in this field, the molecular mechanisms underlying the action of these and other HS loci remain to be elucidated.

In this study, we report the identification and functional characterization of *RHS12*, a locus controlling male gamete sterility in *indica-japonica* inter-subspecific hybrid rice. We show that *RHS12* is composed of two genes (*iORF3*/*DUYAO* and *iORF4*/*JIEYAO*) and that it forms a natural gene drive system. *DUYAO* encodes a toxin that interacts with OsCOX11 to trigger mitochondrial malfunction and cytotoxicity, while *JIEYAO* encodes an antidote to protect the male gametes carrying the *indica*-type *RHS12* allele (*RHS12-i*) via inhibiting DUYAO-OsCOX11 interaction and rerouting DUYAO to the autophagosome for degradation and detoxification, thereby allowing selective transmission of the *RHS12-i* male gamete into the progeny. Our combined results provide insightful understanding into HS and RI in rice and offer broader perspectives on enabling the engineering of such elements for crop breeding or public health purposes.

RESULTS

RHS12 is a major locus affecting male fertility of *indica-japonica* hybrids

To identify previously undescribed genetic components underlying RI between *indica* (genotype denoted as *ii*) and *japonica* (genotype denoted as *jj*) rice, we conducted quantitative trait loci (QTL) analyses of two F_2 populations derived from the F_1 of DJY1 (Dianjingyou 1, a *japonica* variety) × RD23 (an *indica* variety) and the F_1 of T65 (Taichung 65, a *japonica* variety) × G4 (Guangluai 4, an *indica* variety); we detected one and three major QTL controlling rice HS (RHS) in these two F_2 populations, respectively. A major QTL located on chromosome 12 (thus named *RHS12*) was detected in both F_2 populations (Figures S1A and S1B). Notably, this locus is located near several previously identified QTL for RHS between multiple *indica* and *japonica* varieties (*qS12*, *pf12*, *S25*, and *Se*) or between *japonica* and wild rice (*S36*) (Table S1)[28–32]; *RHS12* was thus selected for further study.

To clone the underlying genes of *RHS12*, we generated a near-isogenic line (NIL)-DJY1$^{RD23/RD23}$ in the DJY1 background with the *RHS12*-containing RD23 chromosome segment insertion (Figures S1C and S1D). No obvious difference was observed between the two parents DJY1, NIL-DJY1$^{RD23/RD23}$, and their hybrid F_1 (F_1-DJY1$^{DJY1/RD23}$) in their vegetative and reproductive organs, tapetum degeneration, and formation of tetrads (Figures 1A and S1E–S1G). However, approximately half of the pollen grains of the F_1-DJY1$^{DJY1/RD23}$ plants were sterile (Figure 1B). Further analysis revealed that compared with fertile pollen grains (tricellular at the mature stage), the aborted pollen grains were arrested at the polarized microspore stage, leading to delayed nuclear division, and eventually stopped at the binuclear microspore stage, manifested by insufficient starch accumulation and pollen wall defects (Figure S1H).

Transmission ratio analysis showed that nearly half (49.1%) of the progeny of F_1-DJY1$^{DJY1/RD23}$ pollinated with DJY1 were *DJY1/RD23* heterozygotes (*ij* genotype at the *RHS12* locus) and the other half (50.9%) were *DJY1/DJY1* homozygotes (*jj* genotype) (Figure 1C). However, the majority (91.2%) of the progeny of DJY1 pollinated with F_1-DJY1$^{DJY1/RD23}$ were *DJY1/RD23* heterozygotes, and only 8.8% were *DJY1/DJY1* homozygotes (Figure 1C). The strongly biased transmission of the pollen carrying the *indica*-type *RHS12* allele (*RHS12-i*) and the *japonica* type *RHS12* allele (*RHS12-j*) of F_1-DJY1$^{DJY1/RD23}$ to the progeny indicates that the *RHS12-j* type pollen was selectively aborted and thus failed to transmit into the progeny. Consistent with this pattern, the F_2 population of DJY1 × NIL-DJY1$^{RD23/RD23}$ presented a bimodal distribution for pollen fertility (Figure S2A). Furthermore, segregation of the *RHS12* locus (*ii*:*ij*) in the F_2 population of F_1-DJY1$^{DJY1/RD23}$ fit a 1:1 ratio (Figure S2B), confirming that *RHS12* controls hybrid pollen semi-sterility as a single locus and that the *RHS12-j* type pollen grains of F_1-DJY1$^{DJY1/RD23}$ are selectively eliminated during their transmission to the progeny (Figure S2C).

To fine-map *RHS12*, we initially used an F_2 population with 18,014 individuals derived from the F_1 plants of DJY1 crossed with NIL-DJY1$^{RD23/RD23}$; however, we were only able to narrow down *RHS12* to a 473-kb interval due to a 325-kb chromosomal inversion between the two parents (Figure S2D). Therefore, we switched to an F_2 population derived from T65 × NIL-T65$^{G4/G4}$ (a NIL in the T65 background with the *RHS12*-containing G4 chromosome segment insertion) for fine mapping; this allowed us to delimit *RHS12* to a genomic interval flanked by the molecular markers DK24 and TGR4 (Figures 1D and S2E). Sequence analysis revealed that in T65, the fine-mapping region contains two putative genes (named *jORF1* and *jORF5*), while in G4, besides the genes homologous to *jORF1* and *jORF5* (named *iORF1* and *iORF5*, respectively), it also contains three additional genes, named *iORF2*, *iORF3*, and *iORF4* (Figure 1D).

RHS12 encodes a toxin-antidote system

The genetic architecture of the *RHS12* locus in T65 and G4 bears similarity to several previously reported HS loci in rice that form a killer-protector or toxin-antidote system, such as *S5*, *S1*, and *qHMS7*.[25–27] To test whether *RHS12* encodes a toxin-antidote system, we launched efforts to identify the *ORF*(*s*) that encode a "toxin" and the *ORF*(*s*) that encode an "antidote." We first used the CRISPR-Cas9 technology to individually knockout *iORF1-iORF5* in F_1-T65$^{T65/G4}$. We obtained multiple independent knockout lines for *iORF1*, *iORF2*, *iORF3*, and *iORF5* but failed to

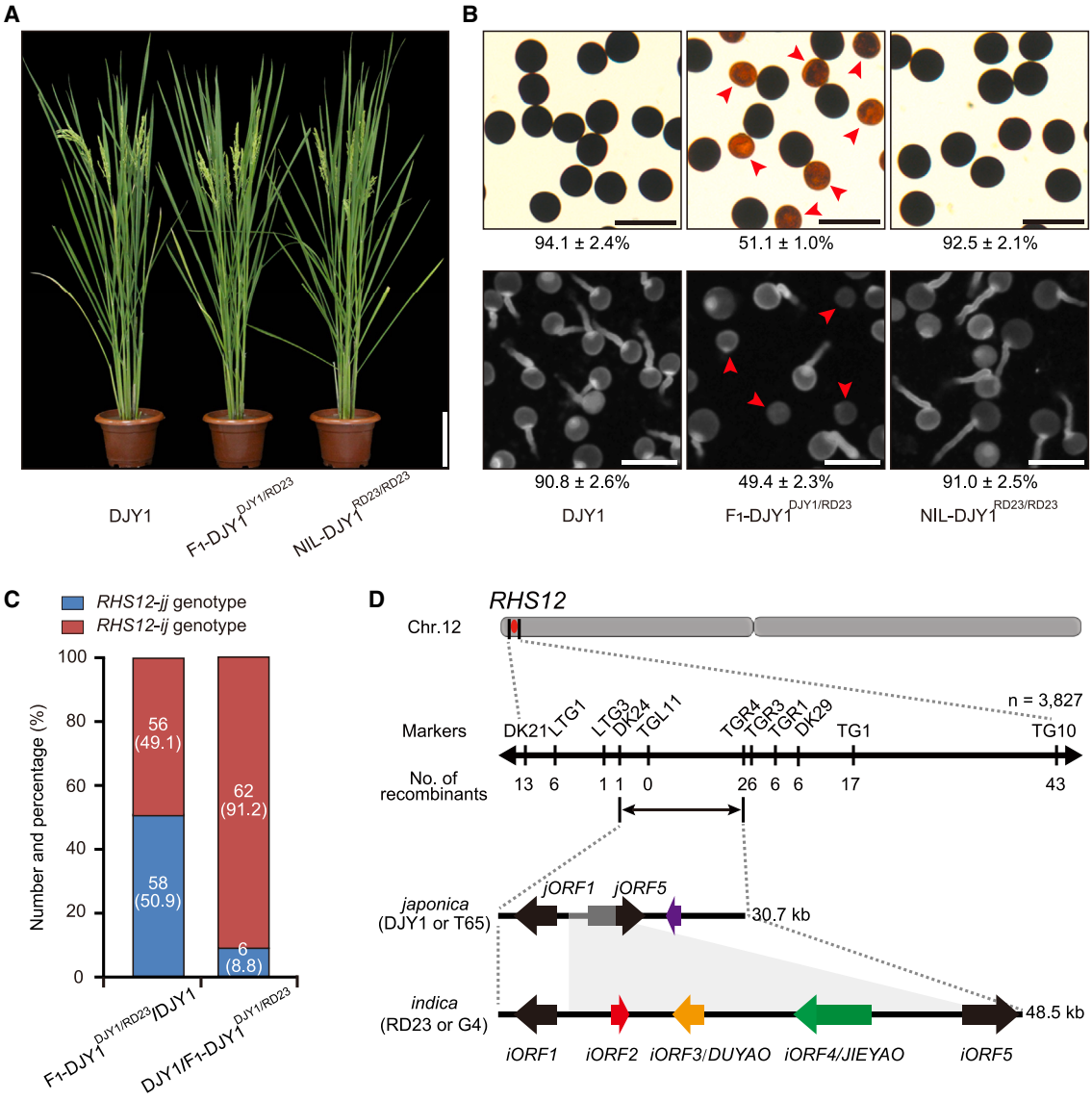

Figure 1. Genetic analyses and cloning of *RHS12*

(A) Plant morphology of DJY1, NIL-DJY1$^{RD23/RD23}$, and their hybrid F_1 (F_1-DJY1$^{DJY1/RD23}$). Scale bars, 20 cm.

(B) I_2-KI staining (top) and germination ability assays (bottom) of pollen grains of DJY1, F_1-DJY1$^{DJY1/RD23}$, and NIL-DJY1$^{RD23/RD23}$ plants. Data are presented as mean ± standard deviation (SD), n = 3 florets. Arrowheads indicate aborted pollen grains. Scale bars, 100 μm.

(C) Number and percentage of the *RHS12-jj* and *RHS12-ij* plants in the hybrid F_1 generation of F_1-DJY1$^{DJY1/RD23}$/DJY1 and DJY1/F_1-DJY1$^{DJY1/RD23}$. *jj* stands for homozygous *DJY1/DJY1* genotype, and *ij* stands for *DJY1/RD23* heterozygous genotype.

(D) Fine mapping of *RHS12*. The transposable element is shown in purple.

See also Figures S1 and S2 and Table S1.

obtain knockout lines for *iORF4* with repeated trials. Fertility analysis revealed that knocking out *iORF1*, *iORF2*, and *iORF5* did not affect the male semi-sterility of F_1-T65$^{T65/G4}$ (Table S1), suggesting that they are not involved in fertility control. In contrast, knocking out *iORF3* fully rescued the male fertility of F_1-T65$^{T65/G4}$. In addition, the segregation ratio of the *RHS12* locus (*jj*:*ij*:*ii*) in the *iORF3* knockout T_1 plants was restored to the expected ratio of 1:2:1 (Figures 2A, 2B, and S2F). These observations suggest that *iORF3* likely encodes a toxin that kills the pollen carrying the *RHS12-j* allele. We therefore renamed it *DUYAO*, which means toxin in Chinese.

The failure to obtain knockout lines for *iORF4* in F_1-T65$^{T65/G4}$ suggested that *DUYAO* might be toxic to somatic cells and that *iORF4* could be required to encode an antidote to protect plant cells from the toxic effect of *DUYAO*. Consistent with this hypothesis, we failed to obtain homozygous knockout lines of *iORF4* in the NIL-T65$^{G4/G4}$ background but obtained homozygous knockout lines of *iORF4* when *DUYAO* was

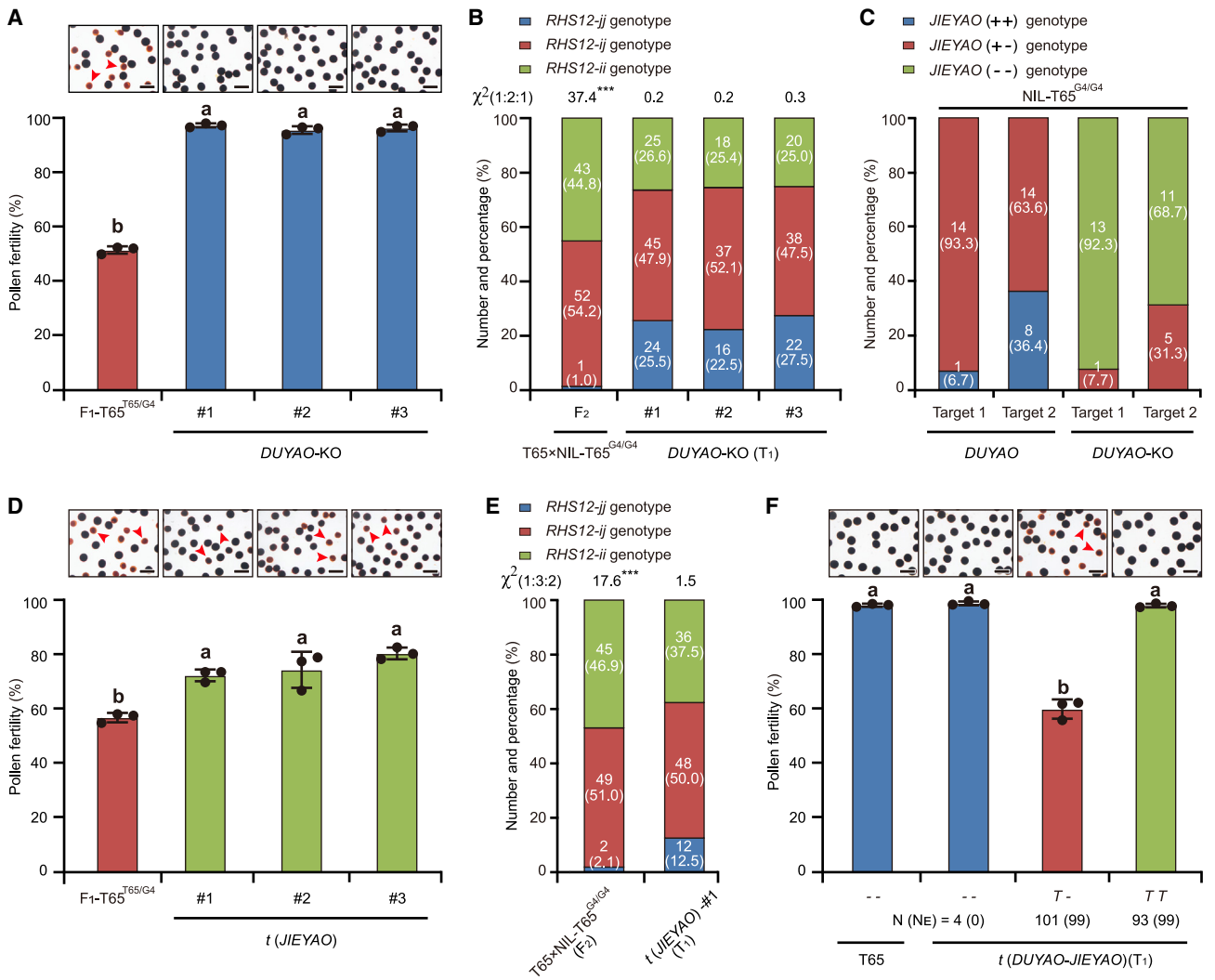

Figure 2. The *DUYAO-JIEYAO* element constitutes a toxin-antidote system

(A) Knocking out *DUYAO* rescues pollen fertility of F_1-T65$^{T65/G4}$. Data are presented as mean ± SD, n = 3 florets. Different letters indicate significant difference at $p < 0.001$ by ANOVA and Tukey's test. Arrowheads indicate aborted pollen grains. Scale bars, 100 μm.

(B) Segregation of *jj*:*ij*:*ii* plants in T65 × NIL-T65$^{G4/G4}$ F_2 population and T_1 progeny of selfed *DUYAO* T_0 knockout plants. Asterisks indicate significant differences (χ^2 test, ***$p < 0.001$).

(C) Number and percentages of various T_0 *JIEYAO*-edited plant types in the NIL-T65$^{G4/G4}$ or its DUYAO-KO backgrounds. Two target sites were designed for knocking out *JIEYAO*. "+" represent wild-type allele and "−" represent mutant allele.

(D) Restoration of pollen fertility of F_1-T65$^{T65/G4}$ carrying single-copy *JIEYAO* transgene. Data are presented as mean ± SD, n = 3 florets. Different letters indicate significant difference at $p < 0.01$ by ANOVA and Tukey's test. Arrowheads indicate aborted pollen grains. Scale bars, 100 μm.

(E) Number and percentage of *jj*:*ij*:*ii* plants from selfed F_1-T65$^{T65/G4}$ carrying single-copy *JIEYAO* transgene. Asterisks indicate significant difference (χ^2 test, ***$p < 0.001$).

(F) Segregation ratio and pollen fertility of T_1 progeny from selfed T_0 plants carrying single-copy *DUYAO-JIEYAO* transgene in T65 background. "*T*" and "−" represent presence or absence of the transgene, respectively. Data are presented as mean ± SD, n = 3 florets. Different letters indicate significant difference at $p < 0.001$ by ANOVA and Tukey's test. Arrowheads indicate aborted pollen grains. Scale bars, 100 μm.

See also Figure S3 and Table S1.

simultaneously knocked out (Figure 2C). To further validate the detoxifying role of *iORF4*, we transformed the genomic region of *iORF4* into F_1-T65$^{T65/G4}$. The pollen fertility of three T_0 single-copy transgenic lines was restored to nearly 75% and the segregation ratio of *jj*:*ij*:*ii* plants in the T_1 generation fits the expected ratio of 1:3:2 (Figures 2D, 2E, and S2G). Further, when we transformed genomic fragments containing *DUYAO* and *iORF4* together into T65, all the hemizygous T_0 transgenic plants were semi-sterile (~50%), and their selfed progeny segregated with an expected ratio of 1:1 for hemizygous (*T*-) and homozygous (*TT*) transgenic plants (Figures 2F and S2H). Together, these observations confirm that *iORF4* indeed encodes an

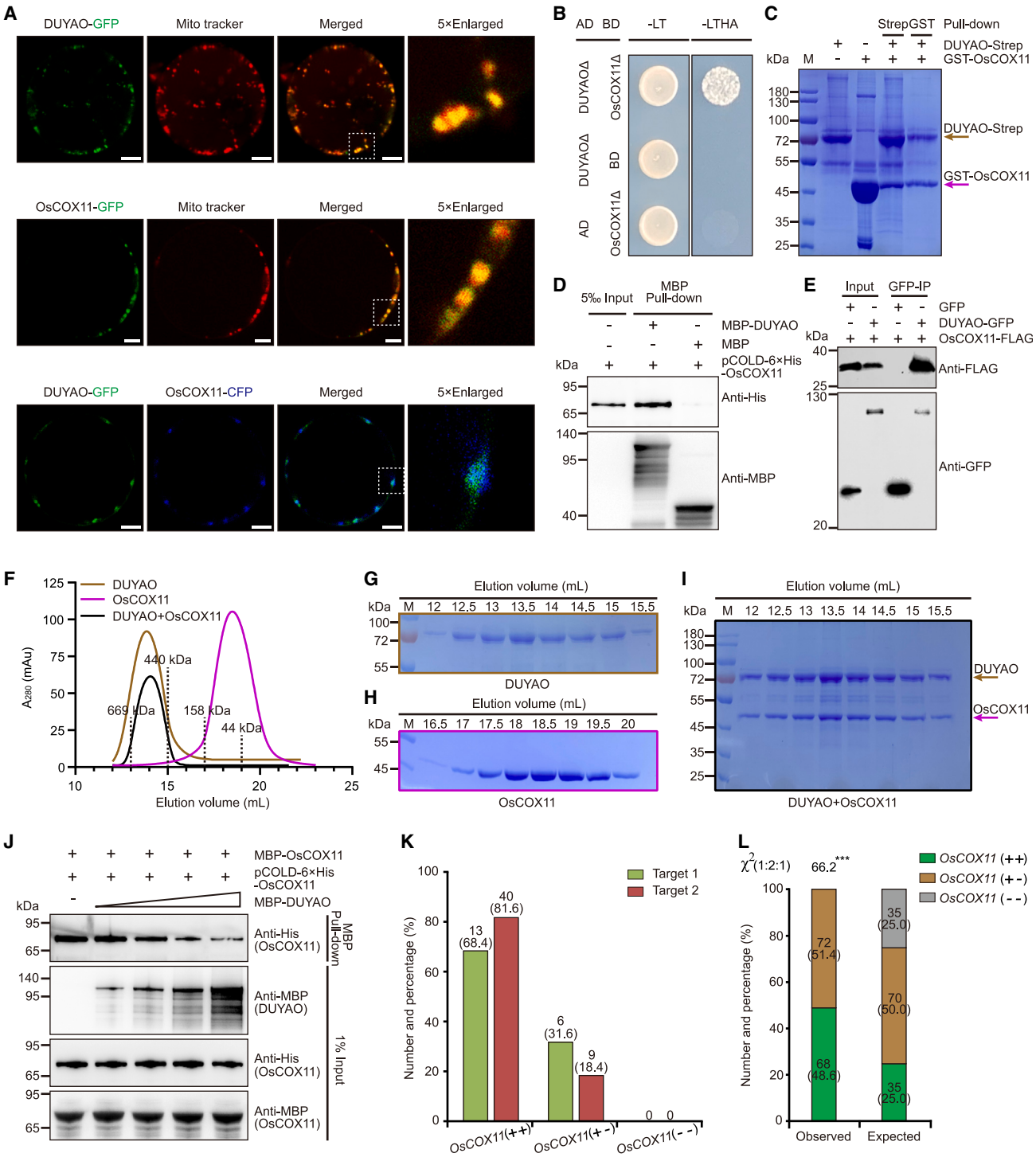

Figure 3. Interaction of DUYAO with OsCOX11

(A) Subcellular localization of DUYAO and OsCOX11 in rice protoplasts. Mito tracker, a specific dye for staining mitochondria. Scale bars, 5 μm.

(B) DUYAO interacts with OsCOX11 in yeast two-hybrid (Y2H) assay. DUYAOΔ and OsCOX11Δ represent their truncated versions without the mitochondria-targeting signal. -LT, synthetic dropout (SD) medium (SD-Leu/-Trp); -LTHA, selective medium (SD-Leu/-Trp/-His/-Ade); AD, active domain; BD, binding domain.

(C) DUYAO interacts with OsCOX11 in pull-down assay. *DUYAO-Strep* and *GST-OsCOX11* were co-expressed in SF21 cells. The DUYAO-OsCOX11 complex was sequentially pulled down by Strep beads and GST beads.

(D) Pull-down of 6×His-OsCOX11 by maltose-binding protein (MBP)-DUYAO, but not by MBP.

(E) Co-immunoprecipitation assay shows that OsCOX11-FLAG could be co-precipitated by DUYAO-GFP.

(legend continued on next page)

antidote to protect the pollen carrying the *RHS12-i* allele. Thus, we renamed *iORF4 JIEYAO*, which means antidote in Chinese.

To further confirm the effect of *DUYAO* and *JIEYAO* in somatic cells, we designed a *p35S::DUYAO-pUbi::GFP* construct and transformed it into T65 calli. Strikingly, we found that the GFP signals disappeared during the callus growing process, implying that *DUYAO* is toxic to calli (somatic cells). By contrast, the GFP signals did not disappear when *DUYAO* and *JIEYAO* were co-infected (Figure S3), supporting a detoxification effect of *JIEYAO* in somatic cells.

DUYAO interacts with OsCOX11 to affect mitochondrial function

To investigate the molecular function of *DUYAO* and *JIEYAO*, we first examined their expression patterns. *RUBY* is a convenient gene expression marker clearly visible to the naked eye.[33] We constructed two *RUBY* reporter genes driven by the promoters of *DUYAO* and *JIEYAO*, respectively. These transgenic plants showed that both *DUYAO* and *JIEYAO* were ubiquitously expressed in all vegetative and reproductive organs examined (Figures S4A–S4H).

Previous studies showed that in the rice wild-abortive cytoplasmic male sterility (WA-CMS) system, the mitochondrial protein WA352 triggers pollen abortion by attacking cytochrome *c* oxidase 11 (OsCOX11), an essential component of the mitochondrial respiratory chain.[34] *DUYAO* is predicted to encode a protein containing a mitochondrial targeting sequence (Figure S5A). A subcellular localization assay revealed that it was localized in the mitochondria in rice protoplasts (Figure 3A). Thus, we speculated that DUYAO might induce mitochondrial malfunction. A subcellular co-localization assay showed that DUYAO was co-localized with OsCOX11 in the mitochondrion (Figure 3A). Furthermore, yeast two-hybrid (Y2H), bimolecular fluorescent complementation (BiFC), pull-down, and co-immunoprecipitation (coIP) assays all demonstrated that DUYAO could directly interact with OsCOX11 (Figures 3B–3E and S5B–S5D). In addition, Y2H, pull-down, and BiFC assays all verified that OsCOX11 could interact with itself (Figures S5E–S5H). Moreover, gel filtration assay showed that OsCOX11 could form homodimeric complex (~80 kDa) as previously reported for yeast COX11,[35] whereas DUYAO could form an oligomeric complex (~650 kDa). When OsCOX11 and DUYAO were co-expressed, OsCOX11 was recruited into the oligomeric complex of DUYAO (Figures 3F–3I), and DUYAO could interfere with homo-dimerization of OsCOX11 (Figure 3J). These results suggest that DUYAO likely exerts a toxic effect on cells via triggering of mitochondrial malfunction by effecting homo-dimerization of OsCOX11.

To further test the role of *OsCOX11* in regulating male fertility, we attempted to knockout *OsCOX11* using the CRISPR-Cas9 technology in T65. We failed to obtain homozygous *Oscox11* knockout plants but obtained heterozygous *OsCOX11* mutant plants. The segregation of heterozygous mutants to non-edited plants in their T_1 generation fits a 1:1 ratio (Figures 3K and 3L). These observations suggest that *OsCOX11* is essential for the survival of both the plant and the male gamete. Taken together, the above results suggest that hybrid pollen sterility induced by *RHS12* is driven by a detrimental interaction between DUYAO and OsCOX11.

JIEYAO detoxifies DUYAO by rerouting it to the autophagosome for degradation

To elucidate the molecular mechanisms of JIEYAO, we first examined whether JIEYAO could physically interact with DUYAO. Y2H, firefly luciferase complementation imaging (LCI), pull-down, and coIP assays all confirmed that full-length proteins of both JIEYAO and DUYAO are critical for their interaction (Figures 4A–4D, S6A, and S6B). Gel filtration assay further showed that JIEYAO and DUYAO could form a heterodimer complex (~160 kDa) and outcompete the formation of the DUYAO oligomers (Figures 4E and 4F). Moreover, coIP assay showed that JIEYAO could overwhelmingly bind to DUYAO and thus abolish the DUYAO-OsCOX11 complex (Figure 4G). These results suggest that JIEYAO could effectively prevent the interaction between DUYAO and OsCOX11.

Next, we used a transient expression system in *Arabidopsis* protoplasts to test the relationship between DUYAO and JIEYAO. DUYAO was localized in mitochondria (Figure S6C), and JIEYAO was localized in the multivesicular body (MVB) and autophagosome when they were expressed alone, respectively (Figure 4H). Intriguingly, when co-expressed with JIEYAO, DUYAO was also localized to the MVB and autophagosome (Figures 4H and 4I). The change of DUYAO's subcellular localization pattern was further verified by exogenously expressing *DUYAO* in rice protoplasts of different genetic backgrounds, including Nipponbare (Nip, a *japonica* variety that lacks an endogenous *DUYAO-JIEYAO* element) and NIL-Nip$^{93\text{-}11/93\text{-}11}$ (a NIL in the Nip background with a fragment containing a functional *DUYAO-JIEYAO* element derived from the *indica* variety 93-11) (Figure S6D).

The autophagosome plays a key role in maintaining cellular homeostasis by mediating degradation of aggregated protein and dysfunctional organelles in the vacuole.[36] A cell-free degradation assay showed that JIEYAO could promote DUYAO degradation *in vitro* and that this process could be inhibited by treatment with the autophagy inhibitor Bafilomycin A1 (BafA1)

(F) Gel filtration assay shows the elution profiles of DUYAO, OsCOX11, and DUYAO-OsCOX11 complexes. Molecular weights are indicated. A_{280}, absorbance at 280 nm; mAu, milli-absorbance units.

(G–I) Coomassie blue staining of SDS-PAGE gel of the peak fractions of DUYAO (G), OsCOX11 (H), and DUYAO-OsCOX11 complex (I) from (F).

(J) Pull-down assay shows that addition of increased amounts of MBP-DUYAO gradually weakens the interaction between MBP-OsCOX11 and 6×His-OsCOX11.

(K) Number and percentage of different edited plant types of *OsCOX11* in T65 background. Two target sites were designed for knocking out *OsCOX11*. "+" represent wild-type allele and "−" represent mutant allele.

(L) Number and percentage of different genotype progeny from selfed heterozygous T_0 *OsCOX11* plants. Asterisks indicate significant difference (χ^2 test, ***$p < 0.001$).

See also Figures S4 and S5.

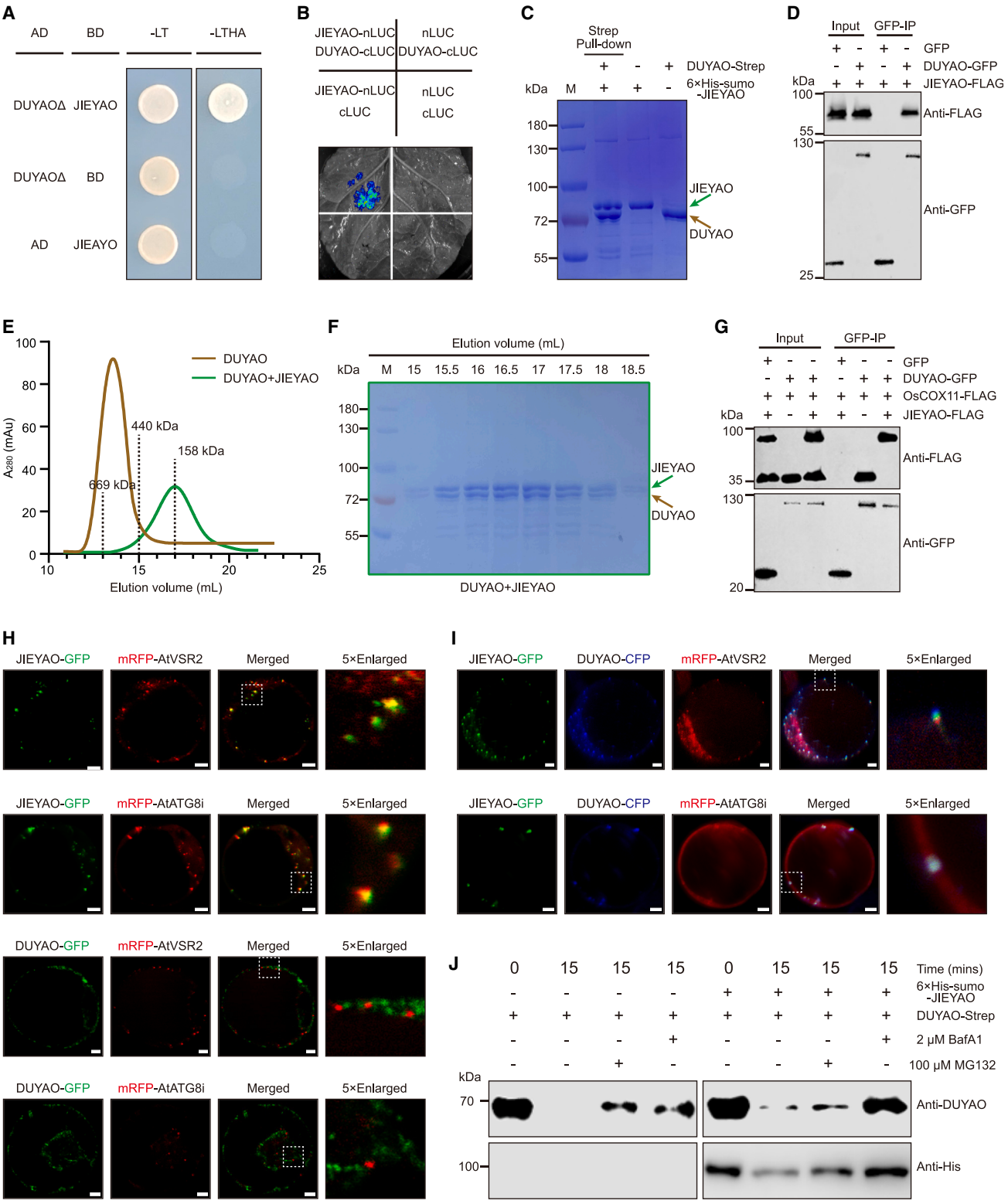

(legend on next page)

(Figure 4J). Together, our data suggest that JIEYAO detoxifies DUYAO via disrupting its oligomerization, rerouting it to the autophagosome for degradation.

Evolutionary trajectory of *RHS12*

To trace the evolutionary origin of the *RHS12* locus, we examined the sequences of *DUYAO* and *JIEYAO* in a diverse sample of 171 wild rice (*O. rufipogon*) and 130 Asian cultivated rice accessions (Table S2). A total of 27 haplotypes of DUYAO and 30 haplotypes of JIEYAO were identified according to nonsynonymous mutations, including amino acid substitutions (designated S) and/or premature stop codons (designated T), respectively, compared with the functional DUYAO and JIEYAO identified in RD23 and G4. These haplotypes of DUYAO and JIEYAO formed a total of 51 haplotype combinations (HCs) in the analyzed samples (Table S2). As functionalization of *JIEYAO* is a prerequisite for the formation of the functional *DUYAO-JIEYAO* element, we first analyzed the possible evolutionary trajectory of *JIEYAO*. Haplotype-1 (Hap-1) of JIEYAO lacks the corresponding sequences, whereas Hap-30 represents the functional JIEYAO as in RD23 and G4 and is characterized by a Lysine residue at the 115th position (denoted as K115). As this residue is present in all functional haplotypes of JIEYAO (Table S2), we thus speculated that K115 might be essential for functionality of JIEYAO. To test this, we conducted CRISPR-Cas9-mediated base-editing technology to change K115 to G115 in NIL-T65$^{G4/G4}$ (Table S3). As expected, we failed to obtain any G115/G115 homozygous lines. All the obtained K115/G115 heterozygous plants (T_0) were semi-sterile (~50%), and the segregation ratio of K115/K115 homozygous and K115/G115 heterozygous plants in the T_1 generation fits a 1:1 ratio (Figure 5A; Table S4), indicating that K115 is essential for functionality of JIEYAO. To further validate the importance of K115 for functionalization of JIEYAO, we constructed a set of NILs with different types of wild and cultivated rice as donors in the DJY1 background to cross with NIL-DJY1$^{RD23/RD23}$ (a test NIL line with functional DUYAO-JIEYAO). The results showed that pollen fertility of the hybrid F_1s (NILs × NIL-DJY1$^{RD23/RD23}$) was fertile (>90%) when the NILs carry JIEYAO^{K115}, differing from those F_1s derived from the NILs lacking JIEYAO or carrying nonsynonymous mutations of K115 in JIEYAO (Figure 5B; Table S5).

Based on the identities of the 115th amino acid residue of JIEYAO, the 30 haplotypes of JIEYAO can be divided into four groups. Hap-1 represents group 1 (lacking the element), while Hap-30 represents group IV (harboring functional JIEYAO). Among the remaining 28 haplotypes, 22 haplotypes belong to group II as their K115 residue is replaced with a glutamine residue (Gln, Q115) or glutamic acid residue (Glu, E115) and thus are nonfunctional; they are hence designated as jieyao^{S}. As jieyao^{S} is nonfunctional, it can be deduced that the duyao$^{S/T}$ in group II is also nonfunctional as this avoids a suicidal combination of the elements. The remaining six haplotypes of JIEYAO (Hap-24 to 29) have K115 but harbor one or more amino acid substitutions at other positions compared with the functional Hap-30 and are hence designated as JIEYAO^{U} (U stands for function undefined). We noticed that Hap-28 and Hap-29 of JIEYAO in group III harbor only one amino acid substitution (L33I or K474T) compared with the functional Hap-30, respectively; thus, we deduced that it is likely from them that the functional JIEYAO is derived (Table S2). Intriguingly, all the rice germplasm of group III haplotypes harbor duyao^{T}, and thus are likely nonfunctional (Table S2). To test this, we created a series of truncated mutants of *DUYAO* in F_1-T65$^{T65/G4}$ using CRISPR-Cas9-mediated base-editing technology (Table S3). Eight pre-termination mutated types of *DUYAO* across the entire coding region were created; as would be predicted for nonfunctional haplotypes, these mutants were fertile (>90%) compared with the semi-sterility (~50%) of F_1-T65$^{T65/G4}$ (Figure 5C).

Based on classification of JIEYAO, the 51 HCs of DUYAO-JIEYAO in our samples could be classified into four groups: group I (HC-1, lacking the *DUYAO-JIEYAO* element), group II (HC-2 to 42), group III (HC-43 to 50), and group IV (HC-51) (Figures 5D and S7A; Table S2). As the sequenced ancestral BB and CC genome wild rice lacks homologous sequences of *DUYAO* and *JIEYAO* (Table S2), we further deduced that the *DUYAO-JIEYAO* element was likely formed *de novo* in AA genome wild rice and is specific to the AA genome clade of the *Oryza* genus. Therefore, we propose that group I (HC-1) likely represents the ancestral form of the *DUYAO-JIEYAO* element, from which group II (HC-2 to -42) arose, and then group III (HC-43 to -50) arose from group II. Finally, the functional group IV (HC-51) was derived from group III, accompanied by functionalization of both *DUYAO* and *JIEYAO* (Figure 5E). Nevertheless,

Figure 4. JIEYAO detoxifies DUYAO by rerouting it to the autophagosome for degradation

(A) Y2H assay shows that JIEYAO interacts with DUYAOΔ.

(B) Firefly luciferase complementation imaging assay shows that JIEYAO interacts with DUYAO in *Nicotiana benthamiana* leaf epidermal cells. nLUC and cLUC denote the N and C terminus of luciferase, respectively.

(C) DUYAO-Strep could pull down 6 × His-sumo-JIEYAO using Strep beads.

(D) Co-immunoprecipitation assay shows that JIEYAO-FLAG could be co-precipitated by DUYAO-GFP.

(E) Gel filtration assay shows that the peak fractions of DUYAO oligomers (~650 kDa) shifted to ~160 kDa DUYAO-JIEYAO heterodimer when JIEYAO was added.

(F) Coomassie blue staining of SDS-PAGE gel shows the separation of DUYAO and JIEYAO of the DUYAO-JIEYAO heterodimeric complex from (E).

(G) Co-immunoprecipitation assay shows that JIEYAO-FLAG could interrupt the interaction between DUYAO-GFP with OsCOX11-FLAG.

(H) Subcellular localization shows that co-localization of JIEYAO-GFP, but not DUYAO-GFP, with mRFP-AtVSR2 (marker for multivesicular body) and mRFP-AtATG8i (marker for autophagosome) in *Arabidopsis* protoplasts. Scale bars, 5 μm.

(I) Subcellular localization assay shows that co-expression of JIEYAO-GFP altered the localization of DUYAO-CFP to the MVB and autophagosome in *Arabidopsis* protoplasts. Scale bars, 5 μm.

(J) Cell-free degradation assay shows that DUAYO-Strep is destabilized by addition of 6 × His-sumo-JIEYAO. BafA1 is an autophagy inhibitor and MG132 is a proteasome inhibitor.

See also Figure S6.

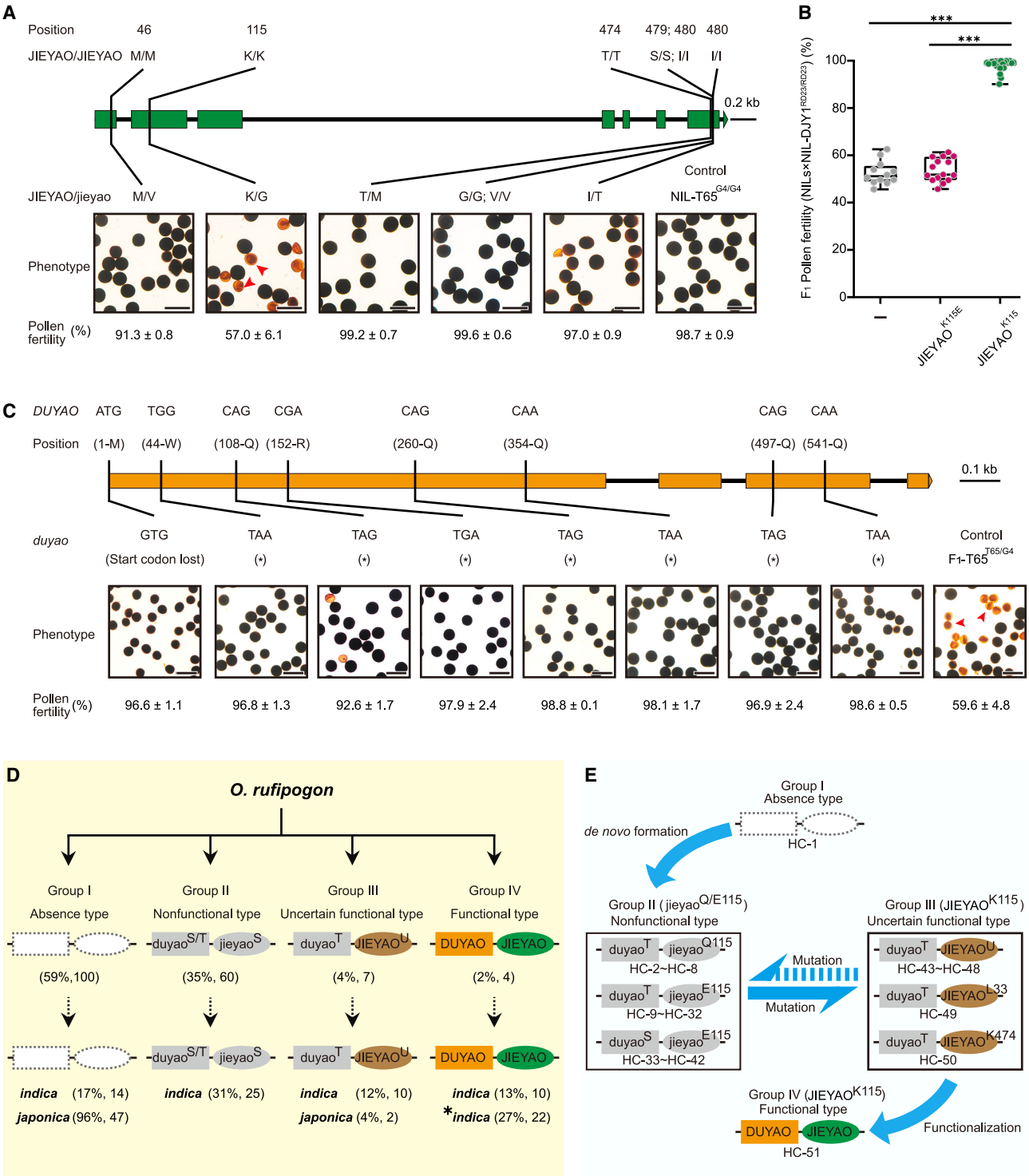

Figure 5. Evolutionary trajectory analysis of the *RHS12* locus

(A) Base editing of *JIEYAO*. The mutated amino acids and corresponding positions in the NIL-T65$^{G4/G4}$ background and the pollen fertility of corresponding transgenic plants are shown. Arrowheads indicate aborted pollen grains. Scale bars, 100 μm.

(B) Pollen fertility of the F_1s (NILs × NIL-DJY1$^{RD23/RD23}$) is normal (>90%) when the NILs carry JIEYAO^{K115}; however, pollen fertility of the F_1s derived from the NILs lacking JIEYAO or carrying nonsynonymous mutations at the 115th amino acid residue of JIEYAO is semi-sterile (~50%). Data are presented as mean ± SD, n = 12, 15, and 24. Asterisks indicate significant difference (χ^2 test, ***p < 0.001).

(legend continued on next page)

other possible evolutionary routes of the *DUYAO-JIEYAO* element may also exist. Notably, the wild rice ancestor *O. rufipogon* contains all four groups of the *DUYAO-JIEYAO* element, and after domestication, only some *indica* rice inherited the functional HC DUYAO-JIEYAO (HC-51) from *O. rufipogon*. Moreover, a chromosome inversion event in group IV *indica* rice appears to have occurred during breeding of cultivated rice (Figures 5D and S2D).

Functional *DUYAO-JIEYAO* element contributes to RI between different lineages of rice

As the functional *DUYAO-JIEYAO* element forms a toxin-antidote system, we deduced that after its initial formation in *O. rufipogon* and its transmission into the *indica* lineage, it could contribute to RI between different populations of wild rice (*O. rufipogon*) and Asian cultivated rice. To test this, we constructed a series of NILs carrying different haplotypes of the *DUYAO-JIEYAO* element in the backgrounds of DJY1, T65, Nip, and Kongyu131 (KY131) and used five of them to make diallel F_1 hybrids. The results showed that F_1 hybrids between NILs carrying functional and nonfunctional *DUYAO-JIEYAO* element were semi-sterile (~50%), whereas F_1 hybrids between NILs carrying nonfunctional *DUYAO-JIEYAO* element were fertile (>90%) (Figures S7B and S7C; Table S5). These observations confirmed that the functional *DUYAO-JIEYAO* element contributed to hybrid male sterility and thus RI between different lineages of rice.

We also noticed that among our sequenced samples, all *japonica* varieties (most of which are landraces) lack the functional *DUYAO-JIEYAO* element. However, most modern *japonica* varieties harbor the functional *DUYAO-JIEYAO* element (see below). Thus, we hypothesized that the functional *DUYAO-JIEYAO* element was likely introgressed into modern *japonica* varieties from *indica* varieties harboring the element during modern rice breeding. To test the functionality of the introgressed *DUYAO-JIEYAO* element, we crossed *japonica* varieties (JG88, H5, and N7) carrying functional *DUYAO-JIEYAO* element with *japonica* varieties (KY131, ZH11, and T65) lacking the element. The resulting F_1 hybrids all displayed male fertility defects, indicating that the introgressed *DUYAO-JIEYAO* element is functional in conferring *de novo* RI in intra-*japonica* varieties (Figure 6A; Table S5).

RHS12 forms a natural gene drive

"Gene drive" is a term coined to describe genetic elements that manipulate gametogenesis and reproduction to increase their own transmission to the next generation.[37,38] To test the gene drive effect of *RHS12* in a natural population, we assessed its frequency change in modern *japonica* rice. No functional *DUYAO-JIEYAO* element was detected in *japonica* landraces before 1970s (Figure 6B; Table S6). Intriguingly, functional *DUYAO-JIEYAO* element (with chromosome inversion) was detected in *japonica* rice varieties registered in China after 1970s, and its frequency increased year by year, reaching 86% in 2019 (Figure 6B; Table S6). These results suggest that the *DUYAO-JIEYAO* element acts as a natural gene drive during the breeding of modern *japonica* varieties.

We further explored whether the *DUYAO-JIEYAO* element could be engineered as an artificial gene drive. We attached *GFP* as an artificial cargo to the *DUYAO-JIEYAO* element and transformed it into T65 calli. T_0 transgenic plants harboring a single-copy *gJIEYAO-pUbi::GFP-gDUYAO* transgene were semi-sterile. Fluorescence microscopy examination revealed that only the *GFP+* pollen grains were fertile, whereas the *GFP−* pollen was aborted (Figures 6C and 6D), suggesting that the *DUYAO-JIEYAO* element could be used to effectively increase transmission of artificial cargo genes.

To further test whether such a gene drive system may work in other species, we constructed a *pADH1::DUYAO* construct and transformed it into yeast (*Saccharomyces cerevisiae*). The results showed that the growth of yeast was significantly inhibited. However, growth of yeast was not affected when transformed with the *pADH1::DUYAOΔ* construct (lacking the mitochondria-targeting signal) or when *pADH1::DUYAO* was co-transformed with *pADH1::JIEYAO* (Figure 6E). Similarly, proliferation of *Drosophila melanogaster* S2 cells was inhibited by transfection of the *DUYAO* construct alone, but not affected when co-transfected with the *DUYAO* and *JIEYAO* constructs (Figure 6F). These results collectively demonstrated that the *DUYAO-JIEYAO* element also functions in other species.

DISCUSSION

In this study, we identified *RHS12* as a major locus controlling hybrid male sterility between different lineages of rice (*indica* and *japonica*) and showed that it encodes a toxin-antidote system. In this system, *DUYAO* acts in a sporophytic manner and encodes a toxin, whereas *JIEYAO* acts in a gametophytic manner and encodes an antidote to protect the male gametes. As a result, the *RHS12-j* pollen grains are selectively eliminated, and the *RHS12-i* pollen is protected by *JIEYAO* and preferentially transmitted to the progeny (Figure 7). Notably, the cytotoxity-detoxification mechanism of *RHS12* bears a similarity to the WA-CMS system in that pollen abortion is caused by mitochondrial malfunction.[34] However, the two systems differ in two major aspects. First, it has been shown that in the WA-CMS system,

(C) Pollen fertility assay shows that different mutations (start codon lost and premature termination) of DUYAO (created via CRISPR-Cas9-mediated base editing) in the F_1-$T65^{T65/G4}$ background rescue pollen fertility. Scale bars, 100 μm.

(D) Deduced evolutionary trajectory of the *RHS12* locus in wild rice ancestor *O. rufipogon* and Asian cultivated rice species. Dotted boxes denote absence of *DUYAO* and *JIEYAO*. The superscript letter S and T indicate amino acid substitutions and pre-termination stop codons, respectively. The superscript letter U indicates function undefined. The percentage and number of accessions of each group are shown in the parenthesis. * denotes the inverted *RHS12* locus found in some *indica* accessions.

(E) A flowchart illustrating the possible evolutionary trajectory of the *RHS12* locus. Four groups of DUYAO-JIEYAO haplotype combinations (HCs) and their possible evolutionary routes are shown.

See also Figure S7 and Tables S2, S3, S4, and S5.

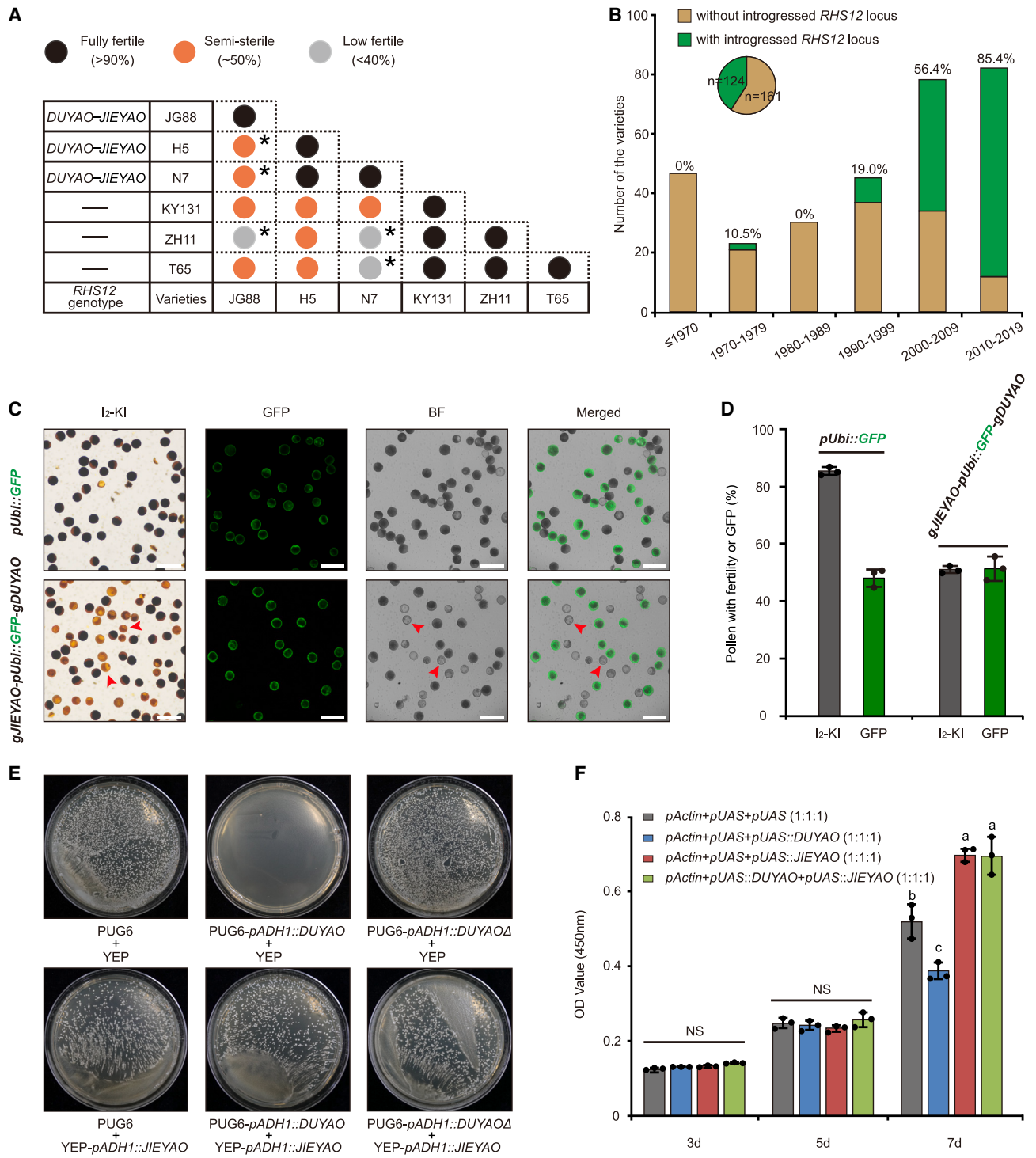

Figure 6. The *DUYAO-JIEYAO* element forms a natural gene drive system

(A) Pollen fertility assay shows that the functional *DUYAO-JIEYAO* element cause hybrid male sterility in diallel crosses between six *japonica* varieties. Heterozygosity at the *RHS12* locus always causes semi-sterile or low-fertile pollen phenotype in the F_1 plants. Asterisks indicate that the lower-than-expected fertility (less than 50%) is caused by other hybrid sterility loci. JG88, Jigeng88; H5, Huaidao 5; N7, Ninggeng 7; KY131, Kongyu131; ZH11, Zhonghua 11.

(B) Spread of the inverted *RHS12* locus in modern *japonica* varieties after its introgression from *indica*. A total of 285 *japonica* varieties were analyzed and the percentage of varieties with introgressed *RHS12* is shown.

(legend continued on next page)

the toxin is caused by WA532-OsCOX11 interaction, which triggers reactive oxygen species and premature programmed cell death of the tapetum cells, leading to pollen abortion.[34] In contrast, in the *DUYAO-JIEYAO* system, cytotoxity is caused by DUYAO-OsCOX11 interaction, which disrupts homo-dimerization and thus proper function of OsCOX11. Second, in the WA-CMS system, detoxification of WA352 is rendered by the nuclear restorer-of-fertility (*Rf*) genes of the restorer lines, which suppress *WA352* expression by cleaving the transcripts of *WA352* or mediating WA352 protein degradation.[34,39] In contrast, in the *DUYAO-JIEYAO* system, JIEYAO detoxifies DUYAO by rerouting it to the autophagosome for degradation through physical interaction. Thus, our study reveals a distinct molecular mechanism underlying hybrid male sterility.

Previous studies have documented ample evidence of the toxin-antidote/meiotic drive/segregation distortion/killer-protector systems as a major form of genetic conflict in different populations of plants and animals to confer RI.[9,10,40] A key feature of such elements (such as the *S5* locus controlling embryo sac fertility of *indica-japonica* hybrid rice, and the *t*-haplotype in mouse controlling sperm motility) is that they usually comprise two or three linked genes encoding a toxin and an antidote.[14,26,41,42] The toxin kills or impairs the development of individuals or gametes while the antidote specifically counteracts the toxin's effects. Thus, such elements are selfish in nature, and they ensure their spread in natural populations by killing the non-carriers, thus subverting Mendel's laws of inheritance. Notably, the tight genetic linkage between the toxin- and antidote-encoding genes in such systems is apparently favored in their evolution, to avoid "suicide" haplotype produced by segregation between the toxin and antidote.[43]

Our evolutionary analyses suggest that the *RHS12* locus is likely formed *de novo* in the AA genome clade of wild rice species (such as *O. rufipogon*) because no homologous sequences of *DUYAO* and *JIEYAO* were identified in BB and CC genome wild rice (Table S2). In addition, we deduced that the functional *DUYAO-JIEYAO* element is likely derived from nonfunctional ancestral *DUYAO-JIEYAO* elements through a multiple-step evolutionary process (amino acid substitutions and removal of premature stop codons). We also demonstrated that once formed, the functional *DUYAO-JIEYAO* element contributed to RI between different lineages/subpopulations of rice that carry it or are non-carriers (Figures 6A, S7B, and S7C). Thus, the *DUYAO-JIEYAO* element likely played a role in promoting RI in cultivated rice by restricting gene flow between different lineages of rice with or without the element.

It is worth noting that all the previously reported *RHS* loci (e.g., *S5*, *qHMS7*, etc.) only affect the male or female gametes,[26,27] whereas *RHS12* acts not only on gametes but also on somatic cells (Figures 6E, 6F, and S3). As in the male gametes, the *DUYAO* of the "*DUYAO-JIEYAO*" element can act as a toxin to disrupt the development and growth of somatic cells, and *JIEYAO* can act as an antidote to relieve the toxic effect of *DUYAO*. The observed effect of the *DUYAO-JIEYAO* element on somatic cells highlights the selfish nature of such elements for their own transmission at the cost of the non-carriers. This system also bears similarity to hybrid necrosis, another form of HI, in that they are all caused by incompatible epistatic interactions between diverged subpopulations of species during evolution. For example, hybrid necrosis in plants is often manifested as a genetic autoimmunity syndrome due to deleterious interaction of functionally diverged nucleotide-binding domain and leucine-rich repeat (NLR) immune receptor genes within or between species.[44,45]

Lastly, our finding that the *DUYAO-JIEYAO* element acts as a natural gene drive suggests broad potential applications. First, we could exploit such a system to generate wide compatibility rice varieties by knocking out *DUYAO* in the *DUYAO-JIEYAO* element to overcome the HS and thereby promote utilization of the strong heterosis between the *indica* and *japonica* subspecies. Second, we also envisage that such an element could be engineered for improving crop breeding efficiency. For example, we could rapidly increase the frequency of genes conferring favorable agronomic traits (such as rice blast gene-*PigmR*, brown planthopper resistance loci-*Bph3* and ideal plant architecture gene-*IPA1*) by linking it to the *DUYAO-JIEYAO* element.[46–48] Third, we can develop pathogen-resistant cultivars using *DUYAO-JIEYAO* element to selectively eliminate the susceptibility genes in a population.[49] Finally, as we showed that the *DUAYO-JIEYAO* gene drive system is functionally conserved in yeast and *Drosophila* somatic cells (Figures 6E and 6F), we also envisage that such a system might be utilized for public health purposes. For example, such a natural gene drive could be engineered to reduce female mosquito transmitted diseases in humans by generating homozygous sterile female mosquitos or male-only populations.[50–53] Indeed, it will be exciting to see such a system fully exploited for biotechnology and biomedical purposes.

Limitations of the study

In this study, we identified *RHS12* as one of the major genetic loci affecting *indica-japonica* hybrid male sterility and demonstrated that this locus encodes a *DUYAO-JIEYAO* element. We revealed that DUYAO induces cytotoxity by affecting mitochondria function, whereas JIEYAO detoxifies it by rerouting it to the autophagosome for degradation. However, several questions remain to

(C) Fluorescence microscopy examination shows that the single-copy transgenic plant of *gJIEYAO-pUbi::GFP-gDUYAO* exhibits a pollen semi-sterile phenotype and presence of the GFP signal in all the fertile pollen grains (lower), whereas in the control single-copy transgenic plants of *pUbi::GFP*, the GFP signal was observed in only half of fertile pollen grains (upper). Arrowheads indicate aborted pollen grains. Scale bars, 100 μm.
(D) Quantification of pollen fertility and presence of GFP signal in (C). Data are presented as mean ± SD, n = 3 florets.
(E) Expression of *DUYAO* alone inhibits yeast growth, but its toxic effect is abolished by co-expressed *JIEYAO*.
(F) Expression of *DUYAO* inhibits proliferation of *Drosophila melanogaster* S2 cells, while co-expression of *JIEYAO* relieved the inhibitory effect of *DUYAO*. Cell density was measured at 3, 5, and 7 days after transfection. Data are presented as mean ± SD, n = 3 trials. Different letters indicate significant differences ($p < 0.05$) by ANOVA and Tukey's test.
See also Tables S5 and S6.

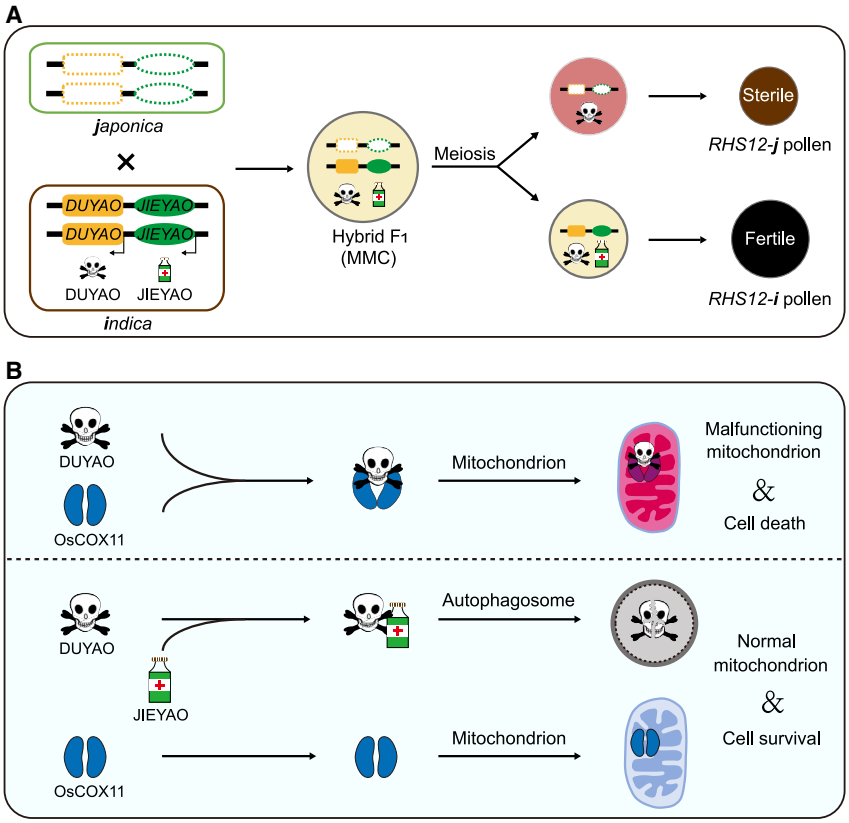

Figure 7. A proposed working model of the *DUYAO-JIEYAO* element acting as a toxin-antidote system

(A) The *RHS12* element acts in a sporo-gametophytic interaction manner to control *indica-japonica* hybrid pollen sterility. After meiosis, two types of pollen grains (*RHS12-i* and *RHS12-j*) were produced. The *RHS12-i* pollen is fertile due to detoxification of DUYAO by JIEYAO. The *RHS12-j* pollen is sterile due to lack of JIEYAO. MMC, microspore mother cell.

(B) DUYAO acts as a toxin by forming a complex with OsCOX11 and blocking its housekeeping function in mitochondria, thus causing cell death. JIEYAO acts as an antidote to protect cells by interacting with DUYAO and rerouting it to the autophagosome for degradation.

be further explored. First, the detailed molecular mechanisms by which JIEYAO acts to alter the subcellular localization of DUYAO from mitochondria to MVBs and autophagosomes remain to be elucidated. Second, the question of how such a system arose in the wild rice progenitors is an interesting issue. The identification of homologous sequences of *DUYAO* and *JIEYAO* only in AA genome wild rice suggests that the *DUYAO-JIEYAO* element likely evolved *de novo* within the AA genome clade of *Oryza*. However, more detailed sequence and functional analyses are required to fully elucidate its origin and evolutionary trajectory in the AA genome species and their close relatives. Lastly, considering that the cytotoxic-detoxification effect of *DUYAO-JIEYAO* element is functionally conserved in yeast and *Drosophila* cells, it will be exciting to see how such an element can be fully exploited for biotechnology and biomedical purposes.

STAR★METHODS

Detailed methods are provided in the online version of this paper and include the following:

- KEY RESOURCES TABLE
- RESOURCE AVAILABILITY
  - Lead contact
  - Materials availability
  - Data and code availability
- EXPERIMENTAL MODEL AND STUDY PARTICIPANT DETAILS
  - Plant materials and growth conditions
  - Microbe strains
- METHOD DETAILS
  - QTL detection and map-based cloning
  - I_2-KI staining, DAPI staining, and DIC examination
  - *In vitro* pollen germination
  - Scanning electron microscopy and transmission electron microscopy
  - Transverse sections of anthers
  - Chromosome behavior observation
  - Complementation assay
  - Knocking out of *DUYAO* and *JIEYAO*
  - Base editing of *DUYAO* and *JIEYAO*
  - "Cytotoxicity-detoxification" effect tested in calli
  - Subcellular localization
  - Yeast two-hybrid (Y2H) assay
  - Bimolecular fluorescent complementation (BiFC) assay
  - Firefly luciferase complementation imaging (LCI) assay
  - Pull-down assay
  - Co-immunoprecipitation (Co-IP) assay
  - Protein purification, pull-down, and gel filtration assays
  - Expression pattern analysis
  - "Cytotoxicity-detoxification" test in yeast
  - S2 cell culture and treatment
  - Evolution and haplotype analysis of the *RHS12* locus

- QUANTIFICATION AND STATISTICAL ANALYSIS
- ADDITIONAL RESOURCES

SUPPLEMENTAL INFORMATION

Supplemental information can be found online at https://doi.org/10.1016/j.cell.2023.06.023.

ACKNOWLEDGMENTS

We thank Xin-Gen Wei, Lihui Zhang, Tianyu Zhang, Xue Yang, Lei Zhou, Ting Yu, Dr. Haiyuan Chen, and Weiyi Kong for help in rice hybridization; Dr. Yao Sun for assistance in rice transformation; Dr. Feng Liu for discussion in subcellular location; Dr. Danting Li and Xiaoping Yuan for providing some wild and cultivated rice accessions. This work was supported by the National Natural Science Foundation of China (32088102, 31991224, 31971909, 31701402, and 31921004), Yunnan Joint Foundation of National Natural Science Foundation (U2002202), National Key R&D Program of China (2022YFD1200801), and the China Postdoctoral Science Foundation (2016M601831 and 2018T110507).

AUTHOR CONTRIBUTIONS

Chaolong Wang, J. Wang, J. Lu, and Y.X. performed most of the experiments and analyzed the data. J. Li, Xiaodong He, C.L., Q.W., Xiaojuan He, B.Y., J.G., X. Zhu, H.Y., Yong Wang, Y.S., H.D., X.G., X.L., Y.T., S.L., Z.C., Ling Jiang, J.Z., and D.T. developed materials and performed genetic analysis. Q.L., Y.R., Y. Zeng, R.M., Y. Zhu, Yunlong Wang, B.H., C.Z., Liwen Jiang, and J.C. performed cytological and biochemical assays. X. Zheng, Y.H., Y. Zhang, W.T., S.C., X.M., and Chunming Wang performed the evolutionary analysis. M.G., B.Z., H.G., and W.Z. performed the experiments in yeast and *Drosophila*. Chaolong Wang, Z.Z., X.Y., C. Wu, H.W., and J. Wan wrote the manuscript. J. Wan conceived and supervised the project.

DECLARATION OF INTERESTS

A patent application (no. 202211059979.0) for the *RHS12* locus and its potential application has been submitted to the State Intellectual Property Office of China.

Received: July 21, 2022
Revised: February 2, 2023
Accepted: June 28, 2023
Published: July 26, 2023

REFERENCES

1. Baack, E., Melo, M.C., Rieseberg, L.H., and Ortiz-Barrientos, D. (2015). The origins of reproductive isolation in plants. New Phytol. *207*, 968–984. https://doi.org/10.1111/nph.13424.
2. Nosil, P., and Schluter, D. (2011). The genes underlying the process of speciation. Trends Ecol. Evol. *26*, 160–167. https://doi.org/10.1016/j.tree.2011.01.001.
3. Orr, H.A., Masly, J.P., and Presgraves, D.C. (2004). Speciation genes. Curr. Opin. Genet. Dev. *14*, 675–679. https://doi.org/10.1016/j.gde.2004.08.009.
4. Rieseberg, L.H., and Blackman, B.K. (2010). Speciation genes in plants. Ann. Bot. *106*, 439–455. https://doi.org/10.1093/aob/mcq126.
5. Fishman, L., and Sweigart, A.L. (2018). When two rights make a wrong: the evolutionary genetics of plant hybrid incompatibilities. Annu. Rev. Plant Biol. *69*, 707–731. https://doi.org/10.1146/annurev-arplant-042817-040113.
6. Johnson, N.A. (2010). Hybrid incompatibility genes: remnants of a genomic battlefield? Trends Genet. *26*, 317–325. https://doi.org/10.1016/j.tig.2010.04.005.
7. Maheshwari, S., and Barbash, D.A. (2011). The genetics of hybrid incompatibilities. Annu. Rev. Genet. *45*, 331–355. https://doi.org/10.1146/annurev-genet-110410-132514.
8. Bravo Núñez, M.A., Nuckolls, N.L., and Zanders, S.E. (2018). Genetic villains: killer meiotic drivers. Trends Genet. *34*, 424–433. https://doi.org/10.1016/j.tig.2018.02.003.
9. Burga, A., Ben-David, E., and Kruglyak, L. (2020). Toxin-antidote elements across the tree of life. Annu. Rev. Genet. *54*, 387–415. https://doi.org/10.1146/annurev-genet-112618-043659.
10. Sweigart, A.L., Brandvain, Y., and Fishman, L. (2019). Making a murderer: the evolutionary framing of hybrid gamete-killers. Trends Genet. *35*, 245–252. https://doi.org/10.1016/j.tig.2019.01.004.
11. Ben-David, E., Burga, A., and Kruglyak, L. (2017). A maternal-effect selfish genetic element in *Caenorhabditis elegans*. Science *356*, 1051–1055. https://doi.org/10.1126/science.aan0621.
12. Dawe, R.K., Lowry, E.G., Gent, J.I., Stitzer, M.C., Swentowsky, K.W., Higgins, D.M., Ross-Ibarra, J., Wallace, J.G., Kanizay, L.B., Alabady, M., et al. (2018). A kinesin-14 motor activates neocentromeres to promote meiotic drive in Maize. Cell *173*, 839–850.e18. https://doi.org/10.1016/j.cell.2018.03.009.
13. Fishman, L., and Saunders, A. (2008). Centromere-associated female meiotic drive entails male fitness costs in monkeyflowers. Science *322*, 1559–1562. https://doi.org/10.1126/science.1161406.
14. Herrmann, B.G., Koschorz, B., Wertz, K., McLaughlin, K.J., and Kispert, A. (1999). A protein kinase encoded by the *t complex responder* gene causes non-Mendelian inheritance. Nature *402*, 141–146. https://doi.org/10.1038/45970.
15. Hu, W., Jiang, Z.D., Suo, F., Zheng, J.X., He, W.Z., and Du, L.L. (2017). A large gene family in fission yeast encodes spore killers that subvert Mendel's Law. eLife *6*, e26057. https://doi.org/10.7554/eLife.26057.
16. Khurana, J.S., Wang, J., Xu, J., Koppetsch, B.S., Thomson, T.C., Nowosielska, A., Li, C., Zamore, P.D., Weng, Z., and Theurkauf, W.E. (2011). Adaptation to *P* element transposon invasion in *Drosophila melanogaster*. Cell *147*, 1551–1563. https://doi.org/10.1016/j.cell.2011.11.042.
17. Merrill, C., Bayraktaroglu, L., Kusano, A., and Ganetzky, B. (1999). Truncated RanGAP encoded by the *Segregation Distorter* locus of *Drosophila*. Science *283*, 1742–1745. https://doi.org/10.1126/science.283.5408.1742.
18. Nuckolls, N.L., Bravo Núñez, M.A., Eickbush, M.T., Young, J.M., Lange, J.J., Yu, J.S., Smith, G.R., Jaspersen, S.L., Malik, H.S., and Zanders, S.E. (2017). *wtf* genes are prolific dual poison-antidote meiotic drivers. eLife *6*, e26033. https://doi.org/10.7554/eLife.26033.
19. Zhang, G.Q. (2020). Prospects of utilization of inter-subspecific heterosis between *indica* and *japonica* rice. J. Integr. Agr. *19*, 1–10. https://doi.org/10.1016/S2095-3119(19)62843-1.
20. Ouyang, Y., and Zhang, Q. (2013). Understanding reproductive isolation based on the rice model. Annu. Rev. Plant Biol. *64*, 111–135. https://doi.org/10.1146/annurev-arplant-050312-120205.
21. Xie, Y., Shen, R., Chen, L., and Liu, Y.G. (2019a). Molecular mechanisms of hybrid sterility in rice. Sci. China Life Sci. *62*, 737–743. https://doi.org/10.1007/s11427-019-9531-7.
22. Koide, Y., Ogino, A., Yoshikawa, T., Kitashima, Y., Saito, N., Kanaoka, Y., Onishi, K., Yoshitake, Y., Tsukiyama, T., Saito, H., et al. (2018). Lineage-specific gene acquisition or loss is involved in interspecific hybrid sterility in rice. Proc. Natl. Acad. Sci. USA *115*. E1955–E1962. https://doi.org/10.1073/pnas.1711656115.
23. Long, Y., Zhao, L., Niu, B., Su, J., Wu, H., Chen, Y., Zhang, Q., Guo, J., Zhuang, C., Mei, M., et al. (2008). Hybrid male sterility in rice controlled by interaction between divergent alleles of two adjacent genes. Proc. Natl. Acad. Sci. USA *105*, 18871–18876. https://doi.org/10.1073/pnas.0810108105.
24. Shen, R., Wang, L., Liu, X., Wu, J., Jin, W., Zhao, X., Xie, X., Zhu, Q., Tang, H., Li, Q., et al. (2017). Genomic structural variation-mediated allelic

suppression causes hybrid male sterility in rice. Nat. Commun. *8*, 1310. https://doi.org/10.1038/s41467-017-01400-y.

25. Xie, Y., Tang, J., Xie, X., Li, X., Huang, J., Fei, Y., Han, J., Chen, S., Tang, H., Zhao, X., et al. (2019b). An asymmetric allelic interaction drives allele transmission bias in interspecific rice hybrids. Nat. Commun. *10*, 2501. https://doi.org/10.1038/s41467-019-10488-3.
26. Yang, J., Zhao, X., Cheng, K., Du, H., Ouyang, Y., Chen, J., Qiu, S., Huang, J., Jiang, Y., Jiang, L., et al. (2012). A killer-protector system regulates both hybrid sterility and segregation distortion in rice. Science *337*, 1336–1340. https://doi.org/10.1126/science.1223702.
27. Yu, X., Zhao, Z., Zheng, X., Zhou, J., Kong, W., Wang, P., Bai, W., Zheng, H., Zhang, H., Li, J., et al. (2018). A selfish genetic element confers non-Mendelian inheritance in rice. Science *360*, 1130–1132. https://doi.org/10.1126/science.aar4279.
28. Kubo, T., Yoshimura, A., and Kurata, N. (2018). Genetic characterization and fine mapping of *S25*, a hybrid male sterility gene, on rice chromosome 12. Genes Genet. Syst. *92*, 205–212. https://doi.org/10.1266/ggs.17-00012.
29. Li, G., Li, X., Wang, Y., Mi, J., Xing, F., Zhang, D., Dong, Q., Li, X., Xiao, J., Zhang, Q., et al. (2017). Three representative inter and intra-subspecific crosses reveal the genetic architecture of reproductive isolation in rice. Plant J. *92*, 349–362. https://doi.org/10.1111/tpj.13661.
30. Liu, B., Li, J.Q., Liu, X.D., Shahid, M.Q., Shi, L.G., and Lu, Y.G. (2011). Identification of neutral genes at pollen sterility loci *Sd* and *Se* of cultivated rice (*Oryza sativa*) with wild rice (*O. rufipogon*) origin. Genet. Mol. Res. *10*, 3435–3445. https://doi.org/10.4238/2011.October.31.10.
31. Win, K.T., Kubo, T., Miyazaki, Y., Doi, K., Yamagata, Y., and Yoshimura, A. (2009). Identification of two loci causing F_1 pollen sterility in inter- and intraspecific crosses of rice. Breed. Sci. *59*, 411–418. https://doi.org/10.1270/jsbbs.59.411.
32. Zhang, H., Zhang, C.Q., Sun, Z.Z., Yu, W., Gu, M.H., Liu, Q.Q., and Li, Y.S. (2011). A major locus *qS12*, located in a duplicated segment of chromosome 12, causes spikelet sterility in an *indica-japonica* rice hybrid. Theor. Appl. Genet. *123*, 1247–1256. https://doi.org/10.1007/s00122-011-1663-z.
33. He, Y., Zhang, T., Sun, H., Zhan, H., and Zhao, Y. (2020). A reporter for noninvasively monitoring gene expression and plant transformation. Hortic. Res. *7*, 152. https://doi.org/10.1038/s41438-020-00390-1.
34. Luo, D., Xu, H., Liu, Z., Guo, J., Li, H., Chen, L., Fang, C., Zhang, Q., Bai, M., Yao, N., et al. (2013). A detrimental mitochondrial-nuclear interaction causes cytoplasmic male sterility in rice. Nat. Genet. *45*, 573–577. https://doi.org/10.1038/ng.2570.
35. Carr, H.S., George, G.N., and Winge, D.R. (2002). Yeast Cox11, a protein essential for cytochrome c oxidase assembly, is a Cu(I)-binding protein. J. Biol. Chem. *277*, 31237–31242. https://doi.org/10.1074/jbc.M204854200.
36. Broda, M., Millar, A.H., and Van Aken, O. (2018). Mitophagy: a mechanism for plant growth and survival. Trends Plant Sci. *23*, 434–450. https://doi.org/10.1016/j.tplants.2018.02.010.
37. Alphey, L.S., Crisanti, A., Randazzo, F.F., and Akbari, O.S. (2020). Opinion: standardizing the definition of gene drive. Proc. Natl. Acad. Sci. USA *117*, 30864–30867. https://doi.org/10.1073/pnas.2020417117.
38. Wedell, N., Price, T.A.R., and Lindholm, A.K. (2019). Gene drive: progress and prospects. Proc. Biol. Sci. *286*, 20192709. https://doi.org/10.1098/rspb.2019.2709.
39. Chen, L., and Liu, Y.G. (2014). Male sterility and fertility restoration in crops. Annu. Rev. Plant Biol. *65*, 579–606. https://doi.org/10.1146/annurev-arplant-050213-040119.
40. Zanders, S.E., and Unckless, R.L. (2019). Fertility costs of meiotic drivers. Curr. Biol. *29*. R512–R520. https://doi.org/10.1016/j.cub.2019.03.046.
41. Bauer, H., Willert, J., Koschorz, B., and Herrmann, B.G. (2005). The t complex-encoded GTPase-activating protein Tagap1 acts as a transmission ratio distorter in mice. Nat. Genet. *37*, 969–973. https://doi.org/10.1038/ng1617.
42. Charron, Y., Willert, J., Lipkowitz, B., Kusecek, B., Herrmann, B.G., and Bauer, H. (2019). Two isoforms of the RAC-specific guanine nucleotide exchange factor TIAM2 act oppositely on transmission ratio distortion by the mouse *t*-haplotype. PLoS Genet. *15*, e1007964. https://doi.org/10.1371/journal.pgen.1007964.
43. Burt, A., and Trivers, R. (2006). Genes in Conflict: the Biology of Selfish Genetic Elements (Harvard University Press). https://doi.org/10.2307/j.ctvjhzrc6.
44. Barragan, A.C., Collenberg, M., Wang, J., Lee, R.R.Q., Cher, W.Y., Rabanal, F.A., Ashkenazy, H., Weigel, D., and Chae, E. (2021). A truncated singleton NLR causes hybrid necrosis in *Arabidopsis thaliana*. Mol. Biol. Evol. *38*, 557–574. https://doi.org/10.1093/molbev/msaa245.
45. Chae, E., Bomblies, K., Kim, S.T., Karelina, D., Zaidem, M., Ossowski, S., Martín-Pizarro, C., Laitinen, R.A., Rowan, B.A., Tenenboim, H., et al. (2014). Species-wide genetic incompatibility analysis identifies immune genes as hot spots of deleterious epistasis. Cell *159*, 1341–1351. https://doi.org/10.1016/j.cell.2014.10.049.
46. Deng, Y., Zhai, K., Xie, Z., Yang, D., Zhu, X., Liu, J., Wang, X., Qin, P., Yang, Y., Zhang, G., et al. (2017). Epigenetic regulation of antagonistic receptors confers rice blast resistance with yield balance. Science *355*, 962–965. https://doi.org/10.1126/science.aai8898.
47. Jiao, Y., Wang, Y., Xue, D., Wang, J., Yan, M., Liu, G., Dong, G., Zeng, D., Lu, Z., Zhu, X., et al. (2010). Regulation of *OsSPL14* by OsmiR156 defines ideal plant architecture in rice. Nat. Genet. *42*, 541–544. https://doi.org/10.1038/ng.591.
48. Liu, Y., Wu, H., Chen, H., Liu, Y., He, J., Kang, H., Sun, Z., Pan, G., Wang, Q., Hu, J., et al. (2015). A gene cluster encoding lectin receptor kinases confers broad-spectrum and durable insect resistance in rice. Nat. Biotechnol. *33*, 301–305. https://doi.org/10.1038/nbt.3069.
49. Tek, M.I., and Budak, K. (2022). A new approach to develop resistant cultivars against the plant pathogens: CRISPR drives. Front. Plant Sci. *13*, 889497. https://doi.org/10.3389/fpls.2022.889497.
50. Alphey, L., McKemey, A., Nimmo, D., Neira Oviedo, M., Lacroix, R., Matzen, K., and Beech, C. (2013). Genetic control of *Aedes* mosquitoes. Pathog. Glob. Health *107*, 170–179. https://doi.org/10.1179/2047773213Y.0000000095.
51. Hammond, A., Galizi, R., Kyrou, K., Simoni, A., Siniscalchi, C., Katsanos, D., Gribble, M., Baker, D., Marois, E., Russell, S., et al. (2016). A CRISPR-Cas9 gene drive system targeting female reproduction in the malaria mosquito vector *Anopheles gambiae*. Nat. Biotechnol. *34*, 78–83. https://doi.org/10.1038/nbt.3439.
52. Kyrou, K., Hammond, A.M., Galizi, R., Kranjc, N., Burt, A., Beaghton, A.K., Nolan, T., and Crisanti, A. (2018). A CRISPR-Cas9 gene drive targeting *doublesex* causes complete population suppression in caged *Anopheles gambiae* mosquitoes. Nat. Biotechnol. *36*, 1062–1066. https://doi.org/10.1038/nbt.4245.
53. Simoni, A., Hammond, A.M., Beaghton, A.K., Galizi, R., Taxiarchi, C., Kyrou, K., Meacci, D., Gribble, M., Morselli, G., Burt, A., et al. (2020). A male-biased sex-distorter gene drive for the human malaria vector Anopheles gambiae. Nat. Biotechnol. *38*, 1054–1060. https://doi.org/10.1038/s41587-020-0508-1.
54. Kumar, S., Stecher, G., Li, M., Knyaz, C., and Tamura, K. (2018). MEGA X: Molecular evolutionary genetics analysis across computing platforms. Mol. Biol. Evol. *35*, 1547–1549. https://doi.org/10.1093/molbev/msy096.
55. Rozas, J., Ferrer-Mata, A., Sánchez-DelBarrio, J.C., Guirao-Rico, S., Librado, P., Ramos-Onsins, S.E., and Sánchez-Gracia, A. (2017). DnaSP 6: DNA sequence polymorphism analysis of large data sets. Mol. Biol. Evol. *34*, 3299–3302. https://doi.org/10.1093/molbev/msx248.
56. Jin, S., Fei, H., Zhu, Z., Luo, Y., Liu, J., Gao, S., Zhang, F., Chen, Y.H., Wang, Y., and Gao, C. (2020). Rationally designed APOBEC3B cytosine base editors with improved specificity. Mol. Cell *79*, 728–740.e6. https://doi.org/10.1016/j.molcel.2020.07.005.

57. Li, C., Zong, Y., Wang, Y., Jin, S., Zhang, D., Song, Q., Zhang, R., and Gao, C. (2018). Expanded base editing in rice and wheat using a Cas9-adenosine deaminase fusion. Genome Biol. *19*, 59. https://doi.org/10.1186/s13059-018-1443-z.

58. Zong, Y., Song, Q., Li, C., Jin, S., Zhang, D., Wang, Y., Qiu, J.L., and Gao, C. (2018). Efficient C-to-T base editing in plants using a fusion of nCas9 and human APOBEC3A. Nat. Biotechnol. *36*, 950–953. https://doi.org/10.1038/nbt.4261.

59. Zhang, Y., Su, J., Duan, S., Ao, Y., Dai, J., Liu, J., Wang, P., Li, Y., Liu, B., Feng, D., et al. (2011). A highly efficient rice green tissue protoplast system for transient gene expression and studying light/chloroplast-related processes. Plant Methods *7*, 30. https://doi.org/10.1186/1746-4811-7-30.

60. Miao, Y., and Jiang, L. (2007). Transient expression of fluorescent fusion proteins in protoplasts of suspension cultured cells. Nat. Protoc. *2*, 2348–2353. https://doi.org/10.1038/nprot.2007.360.

61. Waadt, R., Schmidt, L.K., Lohse, M., Hashimoto, K., Bock, R., and Kudla, J. (2008). Multicolor bimolecular fluorescence complementation reveals simultaneous formation of alternative CBL/CIPK complexes in planta. Plant J. *56*, 505–516. https://doi.org/10.1111/j.1365-313X.2008.03612.x.

62. Miernyk, J.A., and Thelen, J.J. (2008). Biochemical approaches for discovering protein-protein interactions. Plant J. *53*, 597–609. https://doi.org/10.1111/j.1365-313X.2007.03316.x.

STAR★METHODS

KEY RESOURCES TABLE

REAGENT or RESOURCE	SOURCE	IDENTIFIER
Antibodies		
Anti-MBP Monoclonal Antibody	NEB	Cat#E8032L
Anti-His-tag mAb-HRP-DirecT	MBL	Cat#D291-7
Anti-GFP (Green Fluorescent Protein) mAb	MBL	Cat#M048-3
Monoclonal ANTI-FLAG® M2-(HRP) antibody produced in mouse	Sigma-Aldrich	Cat#A8592
Anti-IgG Mouse pAb-HRP	MBL	Cat#330
Anti-IgG Rabbit pAb-HRP	MBL	Cat#458
Rabbit anti-DUYAO	This study	N/A
Bacterial and virus strains		
Agrobacterium tumefaciens EHA105	This study	N/A
*Trans*1-T1 phage Resistant Chemically Competent Cell	TransGen	Cat#CD501-02
Transetta (DE3) Chemically Competent Cell	TransGen	Cat#CD801-02
Saccharomyces cerevisiae strain AH109	This study	N/A
Saccharomyces cerevisiae strain s228c	This study	N/A
DH10Bac Competent Cell	Biomed	Cat#BC112-01
SF21 cells	Thermo Fisher	Cat#B82101
SF9 cells	Thermo Fisher	Cat#B82501
Drosophila Schneider 2 (S2) cells	Invitrogen	Cat#R690-07
Chemicals, peptides, and recombinant proteins		
4', 6-diamidino-2'-phenylindole (DAPI)	Sigma-Aldrich	Cat#D9542-1MG
Propidium Iodide (PI)	Sigma-Aldrich	Cat#P4170-10MG
MitoTracker™ Orange CM-H_2TMRos	Thermo Fisher	Cat#M7511
DO Supplement-Leu/-Trp	Takara	Cat#630417
DO Supplement-His/-Leu/-Trp	Takara	Cat#630419
DO Supplement-Ade/-His/-Leu/-Trp	Takara	Cat#630428
D-Luciferin sodium salt	Solarbio	Cat#D9390
d-Desthiobiotin	Sigma-Aldrich	Cat#D1411
HyClone SFX-Insect	HyClone	Cat#SH30278.02
Fetal Bovine Serum (FBS)	Gibco	Cat#10099141
Critical commercial assays		
QIAGEN Plasmid Midi Kit (25)	QIAGEN	Cat#12143
Yeastmaker™ Yeast Transformation System 2	Takara	Cat#630439
Amylose resin	NEB	E8021S
Anti-GFP mAb-Magnetic agarose	MBL	Cat#D153-11
Streptactin Beads 4FF	Smart-Lifesciences	Cat#SA053025
Chelating sepharose fast flow	GE Healthcare	Cat#17-0575-02
Glutathione Sepharose 4B	GE Healthcare	Cat#17-0756-04
In-Fusion HD® Cloning Kit	Takara	Cat#639650
2X MultiF Seamless Assembly Mix	ABclonal	Cat#RK21020
KOD FX	TOYOBO	Cat#KFX-101
Phanta Max Super-Fidelity DNA Polymerase	Vazyme	Cat#P505-d1

(*Continued on next page*)

Continued

REAGENT or RESOURCE	SOURCE	IDENTIFIER
Effectene Transfection Reagent	QIAGEN	Cat#301425
Cell Counting kit-8(CCK-8)	APExBIO	Cat#K1018
Experimental models: Organisms/strains		
Nicotiana benthamiana	This study	N/A
Rice: *Oryza sativa* ssp. *japonica* Taichung 65, T65	This study	N/A
Rice: *Oryza sativa* ssp. *indica* Guangluai 4, G4	This study	N/A
Rice: *Oryza sativa* ssp. *japonica* Dianjingyou 1, DJY1	This study	N/A
Rice: *Oryza sativa* ssp. *indica* RD23	This study	N/A
Rice: NILs, NIL-T65$^{G4/G4}$, NIL-DJY1$^{RD23/RD23}$	This study	N/A
Rice: Hybrid F_1, T65/G4	This study	N/A
Rice: Hybrid F_1, DJY1/RD23	This study	N/A
Rice: Hybrid F_1, F_1-T65$^{T65/G4}$	This study	N/A
Rice: Hybrid F_1, F_1-DJY1$^{DJY1/RD23}$	This study	N/A
Rice: *Oryza sativa* ssp. *japonica* Nipponbare	This study	N/A
Rice: *Oryza sativa* ssp. *indica* 93-11	This study	N/A
Rice: F_1-T65$^{T65/G4}$/DUYAO-KO	This study	N/A
Rice: F_1-T65$^{T65/G4}$/*JIEYAO*	This study	N/A
Rice: T65/*DUYAO-JIEYAO*	This study	N/A
Rice: F_1-T65$^{T65/G4}$/*DUYAO*-Base editing-1∼8	This study	N/A
Rice: NIL-T65$^{G4/G4}$ /*JIEYAO*-KO-1/2	This study	N/A
Rice: NIL-T65$^{G4/G4}$ /*JIEYAO*-Base editing-1∼5	This study	N/A
Rice: T65/*OsCOX11*-KO	This study	N/A
Rice: T65/*pDUYAO::RUBY*	This study	N/A
Rice: T65/*pJIEYAO::RUBY*	This study	N/A
Rice: T65/*pUbi::GFP*	This study	N/A
Rice: T65/*gJIEYAO-pUbi::GFP-gDUYAO*	This study	N/A
Recombinant DNA		
CRISPR-*DUYAO*	This study	N/A
2300-*JIEYAO*	This study	N/A
2300-*DUYAO-JIEYAO*	This study	N/A
2300-*pUbi::GFP*	This study	N/A
2300-*p35S::DUYAO-pUbi::GFP*	This study	N/A
2300-*pActin::JIEYAO*	This study	N/A
2300-*pActin::JIEYAO-pUbi::GFP-p35S::DUYAO*	This study	N/A
2300-*gJIEYAO-pUbi::GFP-gDUYAO*	This study	N/A
2300-*pUbi::GFP-gJIEYAO-gDUYAO*	This study	N/A
CRISPR-*DUYAO*-Base editing-1∼8	This study	N/A
CRISPR-*JIEYAO*-1/2	This study	N/A
CRISPR-*JIEYAO*-Base editing-1∼5	This study	N/A
DUYAO-GFP	This study	N/A
OsCOX11-GFP	This study	N/A
JIEYAO-GFP	This study	N/A
DUYAO-CFP	This study	N/A

(*Continued on next page*)

Continued

REAGENT or RESOURCE	SOURCE	IDENTIFIER
OsCOX11-CFP	This study	N/A
1390-*pUbi::JIEYAO*	This study	N/A
pGADT7-DUYAOΔ	This study	N/A
pGADT7-DUYAO-D1∼D5	This study	N/A
pGADT7-OsCOX11Δ	This study	N/A
pGBKT7-OsCOX11Δ	This study	N/A
pGBKT7-OsCOX11-D1∼D4	This study	N/A
pGBKT7-JIEYAO	This study	N/A
pGBKT7-JIEYAO-D1∼D5	This study	N/A
p2YC-DUYAO	This study	N/A
p2YN-OsCOX11	This study	N/A
p2YC-OsCOX11	This study	N/A
MBP-DUYAO	This study	N/A
MBP-OsCOX11	This study	N/A
pCOLD-His-OsCOX11	This study	N/A
1390-*pUbi::OsCOX11-3×FLAG*	This study	N/A
1390-*pUbi::JIEYAO-3×FLAG*	This study	N/A
DUYAO-cLUC	This study	N/A
JIEYAO-nLUC	This study	N/A
pDUYAO::RUBY	This study	N/A
pJIEYAO::RUBY	This study	N/A
pUASTattB	This study	N/A
pActin::Gal4	This study	N/A
pUAS::DUYAO	This study	N/A
pUAS::JIEYAO	This study	N/A
YEB-*pADH1::JIEYAO*	This study	N/A
PUG6-pADH1::*DUYAO*	This study	N/A
PUG6-pADH1::*DUYAOΔ*	This study	N/A
pFastBac-His-sumo-JIEYAO-1-451	This study	N/A
pFastBac-DUYAO-Strep	This study	N/A
pFastBac-GST-OsCOX11	This study	N/A
Software and algorithms		
QTL IciMapping Version 4.2	ICS-CAAS	https://isbreeding.caas.cn/rj/qtllcampping/
Adobe Photoshop CS6	Adobe	https://www.adobe.com/cn/products/photoshop.html
Adobe Illustrator	Adobe	https://www.adobe.com/cn/products/illustrator.html
GraphPad Prism 8	GraphPad	https://www.graphpad.com/scientific-software/prism/
MEGAX	Kumar et al.[54]	https://www.megasoftware.net
DnaSP6	Rozas et al.[55]	http://www.ub.edu/dnasp/

RESOURCE AVAILABILITY

Lead contact

Further information and requests for resources and reagents should be directed to and will be fulfilled by the lead contact, Jianmin Wan (wanjianmin@caas.cn or wanjm@njau.edu.cn).

Materials availability

Constructs, strains, NILs, and transgenic seeds generated in this study will be made available upon request for scientific research while a completed Materials Transfer Agreement should be required if there is potential for commercial application.

Data and code availability

- The nucleotide sequences of *DUYAO* (OQ351923) and *JIEYAO* (OQ351924) described in this study have been deposited in the GenBank database.
- This study did not generate any code.
- Any additional information required to reanalyze the data reported in this paper is available from the lead contact upon request.

EXPERIMENTAL MODEL AND STUDY PARTICIPANT DETAILS

Plant materials and growth conditions

Two F_2 populations derived from *japonica/indica* crosses (including T65 × G4 and DJY1 × RD23) were used for QTL detection. NILs, including NIL-DJY1$^{RD23/RD23}$, NIL-T65$^{G4/G4}$ and those from other donors in DJY1, Nipponbare or KY131 background were used for genetic analysis. Besides T65, NIL-T65$^{G4/G4}$ and F_1-T65$^{T65/G4}$ were also used for genetic transformation. *japonica* variety Nipponbare and *indica* variety 93-11 seedlings were cultured *in vitro* for rice protoplast preparation. All the wild-type and transgenic plants for phenotype observation were grown in paddy field in Nanjing (118°E, 32°N) in summer or Hainan Island (110°E, 18°N) in winter.

Nicotiana benthamiana for BiFC and LCI assays was grown at 22°C under long-day condition (16-h day/8-h night) and 4∼5 weeks old leaves were collected for transient expression assays.

Microbe strains

The *Saccharomyces cerevisiae* strains AH109 and s228c were stored at -70°C, and re-activated by culturing in an incubator at 30°C for 3 days before use.

METHOD DETAILS

QTL detection and map-based cloning

For QTL detection of hybrid pollen sterility loci, two F_2 populations of *indica* × *japonica* hybrid rice were used, one derived from T65 × G4 containing 116 individuals that were genotyped by 204 markers, another derived from DJY1 × RD23 including 156 individuals that were genotyped by 142 markers. The pollen fertility of individuals was examined by I_2-KI staining and QTL analysis was performed using the QTL IciMapping Version 4.2 software.

The *RHS12* locus was first mapped to a 473-kb region on the short arm of chromosome 12 between InDel markers NJ5 and G8 using the DJY1 × NIL-DJY$^{RD23/RD23}$ F_2 population with 18,014 individuals. There were no recombinant individuals inside the region as it contains an inversion structure. Then, 3,827 individuals generated from another F_2 population of T65 × NIL-T65$^{G4/G4}$ (without the inversion structure) were used for fine mapping and the mapped region was finally narrowed down to a 30.7-kb interval between InDel markers DK24 and TGR4. To verify *RHS12* within this interval, pollen fertility and genotypic $F_{2:3}$ segregation ratio of recombinant individuals were investigated for consistence.

I_2-KI staining, DAPI staining, and DIC examination

Pre-flowering spikelets were fixed in Carnoy's solution (ethanol: glacial acetic=3:1) and then stored at 4°C before observation. For microscopic examination, pollen grains were released from anthers using tweezers and then stained by 1% I_2-KI solution.

For DAPI staining, pre-flowering spikelets were fixed in FAA solution (70% ethanol: formalin: acetic acid=18:1:1) and then stored at 4°C before examination. Released pollen grains were stained for 20 min by DAPI solution (1 μg/mL), and a drop of 40% glycerinum was added before being photographed with ZEISS Imager A2 fluorescence microscope.

Fresh anthers at different developmental stages of F_1-DJY1$^{DJY1/RD23}$ were collected and then the pollen grains were released in 1% sucrose solution before photographing using DIC microscope.

In vitro pollen germination

To observe the *in vitro* pollen germination ability, on the day of filaments elongation and pollen grains dispersal, parental and hybrid F_1 pollen grains were collected by gently shaking pollen grains into the germination solution (10% sucrose, 0.1 mg/mL H_3BO_3, and 0.1 mg/mL Ca $(NO_3)_2$). The slide loaded with the germination solution was then cultured at 30°C for 15∼20 min in darkness, followed by adding one drop of 0.005% aniline blue solution before imaging.

Scanning electron microscopy and transmission electron microscopy

To conduct scanning electron microscopy, mature anthers were first fixed in 2.5% glutaraldehyde for 24 h, rinsed 3 times using distilled water, dehydrated through an ethanol series, then fixed in 1% OsO_4 for 2 h, and dehydrated through ethanol series again followed by critical point drying with CO_2. After that, the anthers were coated with gold by E-100 ion sputter and then observed using scanning electron microscopy (S3400, Hitachi).

For transmission electron microscopy, anthers were fixed in 2.5% glutaraldehyde as aforementioned, rinsed twice by 0.1 mol/L phosphate buffered saline (PBS) solution, 30 min each, and then dehydrated through acetone series, followed by treatment with

saturated uranium acetate prepared with 70% acetone at 4°C overnight. After that, the anthers were embedded in epoxy resin, and then kept at three temperature gradients of 37°C for 12 h, 45°C for 24 h, and 60°C for 24 h. The ultrathin sections of 60-70 nm were then double stained with 2% (w/v) uranyl acetate and 2.6% (w/v) aqueous lead citrate solution. The sections were observed by a JEM-1230 transmission electron microscope (JEOL) at 80kV.

Transverse sections of anthers

Spikelets at different developmental stages were fixed in 2.5% glutaraldehyde for 12 h and rinsed twice with 0.1 M PBS solution, 30 min each, followed by dehydration through acetone series. The samples were then permeated with resin that was diluted with 25%, 50%, and 75% anhydrous acetone, each for 3 h at room temperature, and finally with 100% resin for one week at 35°C. At last, the samples were polymerized at 60°C for 48 h before slicing. The sections of approximate 1 μm thick were stained by 0.5%-1% toluidine blue. Photos were taken with Olympus BX43 microscope and enhanced by Adobe Photoshop CS6 software.

Chromosome behavior observation

Young panicles during meiosis were collected and fixed in Carnoy's solution at 4°C before use. At first, one anther of the spikelet was stained by aceto carmine to precisely determine the phases of meiosis. Anthers at desired phase were squashed under a cover slip in 40% acetic acid. After that, the slide was immersed in liquid nitrogen for 15 min; then the cover slip was removed quickly, followed by dehydration with 70%, 90%, and 100% ethanol. At last, the slide was dried at room temperature for 5 min before staining by PI (20 μg/mL). Images were captured using ZEISS Imager A2 fluorescence microscope and then enhanced by Adobe Photoshop CS6 software.

Complementation assay

For investigating the role of *JIEYAO* at the *RHS12* locus, genomic sequence of *JIEYAO* driven by *Actin* promotor was amplified and inserted into pCAMBIA2300 to generate 2300-*pActin*::*JIEYAO* construct. Then the construct was transformed into F_1-$T65^{T65/G4}$ calli via *Agrobacterium tumefaciens*-mediated transformation. Single-copy transgenic T_0 plants were examined to see if pollen fertility was rescued to about 75% and if their progeny T_1 plant followed the segregation ratio of 1:3:2 (*jj*:*ij*:*ii*) at the *RHS12* locus.

To clarify the role of *DUYAO-JIEYAO* as a selfish element, a 20-kb genomic DNA fragment spanning *DUYAO* and *JIEYAO* was amplified and cloned into pCAMBIA2300 to generate 2300-*DUYAO-JIEYAO* construct. The construct was then transformed into T65 calli. Then, the transgenic plants were sequenced and analyzed to identify T-DNA integration site and to facilitate T_1 segregation ratio determination. Corresponding pollen phenotype and segregation ratio in T_1 generation derived from single copy T_0 plant were investigated. Primers used for amplification are listed in Table S7.

Knocking out of *DUYAO* and *JIEYAO*

An 18-bp length sequence targeting *DUYAO* was synthesized, annealed and subsequently cloned into the CRISPR/Cas9 vector. The CRISPR-*DUYAO* construct was then transformed into F_1-$T65^{T65/G4}$ calli and edited plants were identified by polymerase chain reaction (PCR)-based sequencing. The *DUYAO* knockout plants were chosen to investigate pollen fertility and T_1 segregation ratio.

To create *JIEYAO* knockout plants using the CRISPR/Cas9 technology, sequences targeted to two targets (target1 and target2) were designed. The resulting constructs were transformed into F_1-$T65^{T65/G4}$ (with heterozygous *DUYAO*), NIL-$T65^{G4/G4}$ (with homozygous *DUYAO*), and NIL-$T65^{G4/G4}$-KO (with *DUYAO* knocked out). Transgenic plants were genotyped by PCR-based sequencing with *JIEYAO*-specific primers to determine possible mutations at the targets. Primers used for amplification are listed in Table S7.

Base editing of *DUYAO* and *JIEYAO*

To create point mutations of *DUYAO* and *JIEYAO*, we generated several base editors by replacing deaminase and Cas9 portions of former plant adenine base editor and cytosine base editor constructs,[56–58] yielding pH-ABE8e-NG-esgRNA, pH-ABE8e-SpRY-esgRNA, pH-A3A-CBE-NG, and pH-VHM-NG. The original TadA8e deaminase was optimized with cereal-preferred codons and synthesized commercially (GenScript); the Cas9 PAM variants (recognizing relaxed PAM) were amplified and mutated from corresponding constructs by PCR. All the deaminase and Cas9 portions were installed using 2×MultiF Seamless Assembly Mix (ABclonal). The annealed sgRNA oligos were then installed into corresponding constructs by Golden Gate. The resulting constructs were transformed into F_1-$T65^{T65/G4}$ and NIL-$T65^{G4/G4}$ calli by *Agrobacterium*-mediated transformation. The target sequences are listed in Table S3.

"Cytotoxicity-detoxification" effect tested in calli

To investigate the role of *DUYAO-JIEYAO* element in somatic cells, constructs consisting of different elements were transformed into T65 calli. GFP driven by *Ubi* promoter (2300-*pUbi::GFP*) was used as a negative control and transgenic calli surviving selection were expected to show bright GFP signal. With addition of *DUYAO* driven by the *35S* promoter (2300-*p35S*::*DUYAO-pUbi::GFP*), GFP signal would diminish in transgenic cells along with accumulation of DUYAO (if it is toxic). With further addition of *JIEYAO* driven by the *Actin* promoter (2300-*pActin*::*JIEYAO-pUbi*::*GFP-p35S::DUYAO*), bright GFP was expected in transgenic calli due to presence of JIEYAO (if it exerts detoxification). An accompanying construct 2300-*pActin::JIEYAO* was also made as another control. Alternatively, 2300-*p35S*::*DUYAO-pUbi::GFP* and 2300-*pActin::JIEYAO* were co-transformed into T65 calli using

Agrobacterium-mediated method as a supporting test. Besides, native promoters were also used to generate 2300-*gJIEYAO-pUbi*::*GFP-gDUYAO* and 2300-*pUbi*::*GFP-gJIEYAO-gDUYAO* vectors. GFP signal was observed two weeks (with hygromycin selection) after *Agrobacterium* infection. Images were captured with Leica M205 FCA stereo fluorescence microscope, and then enhanced using Adobe Photoshop CS6 software. Primers used for amplification are listed in Table S7.

Subcellular localization

The coding region of *DUYAO*, *OsCOX11*, and *JIEYAO* were amplified and then fused with *GFP* and *CFP* to generate *DUYAO-GFP*, *OsCOX11-GFP*, *JIEYAO-GFP*, *DUYAO-CFP*, and *OsCOX11-CFP* constructs, respectively. All the fused genes were under the control of double *35S* promoter, except in 1390-*pUbi*::*JIEYAO* where *JIEYAO* was driven by the maize *Ubiquitin*-1 promoter for transient expression of JIEYAO without tag. Leaf sheaths of two week-old Nipponbare and 93-11 seedlings were used to isolate protoplasts. The leaf sheaths were cut into strips of 0.5 mm in length, treated with 0.6 M mannitol and then incubated in an enzyme solution (0.75% macerozyme R-10, 1.5% cellulase RS, 0.1% bovine serum albumin, 0.6 M mannitol, 10 mM 2-(N-Morpholino) ethanesulfonic acid (MES) at pH 5.7 and 10 mM $CaCl_2$) in dark for 4 h with gentle shaking. Protoplasts released from cell wall digestion were collected by centrifugation and transfected with plasmid DNA representing various construct combinations via the polyethyleneglycol-mediated procedure.[59] Transient gene expression in protoplasts prepared from the *Arabidopsis* PSB-D cell culture[60] was performed as the followings. The *Arabidopsis* cells (3-5 days in subculture) were incubated in an enzyme solution (1% cellulose RS, 0.05% pectinase, 0.2% driselase, 0.4 M sucrose, 4.3 g/L Murashige and Skoog salts, 500 mg/L MES hydrate, 750 mg/L $CaCl_2.2H_2O$ and 250 mg/L NH_4NO_3, pH 5.7) on a shaker at 65 rpm under 25°C for 2.5-3 h. The isolated protoplasts were collected and washed using electroporation buffer (0.4 M sucrose, 2.4 g/L 4-(hydroxyethyl)-1-piperazineethanesulfonic acid, 6 g/L KCl and 600 mg/L $CaCl_2.2H_2O$, pH 7.2) twice before electroporation with 40 μg plasmid DNA mix representing different construct combinations. After incubation at 26°C for 6-18 h, the protoplasts were observed for fluorescent signals. Autophagosomes were induced by 100 μM benzothiadiazole (BTH) for 6-8 h. Mitochondria were stained by MitoTracker™ Orange CM-H_2TMRos and fluorescence of protoplasts were observed and imaged using a confocal laser scanning microscope (Leica SP8). Primers used for amplification are listed in Table S7.

Yeast two-hybrid (Y2H) assay

The coding region of *JIEYAO*, mitochondrial signal-less *DUYAO* (*DUYAOΔ*) and *OsCOX11* (*OsCOX11Δ*), and their fragmented versions (*JIEYAO-D1∼D5* for *JIEYAO*, *DUYAO-D1∼D5* for *DUYAO* and *OsCOX11-D1∼D4* for *OsCOX11*) were amplified and then cloned into Y2H prey vector pGADT7 or pGBKT7 (Clontech). The resulting constructs were co-transformed in various combinations into *Saccharomyces cerevisiae* strain AH109 according to the manufacture's instruction (Yeastmaker™ Yeast Transformation System 2). The transfected yeast cells were first grown on synthetic dropout medium (SD-Leu/-Trp) at 30°C for 3 days and then transferred to selective medium (SD-Leu/-Trp/-His/-Ade) at 30°C for 4 days. Primers used for amplification are listed in Table S7.

Bimolecular fluorescent complementation (BiFC) assay

For BiFC assay, the full-length coding region of *DUYAO* and *OsCOX11* were amplified and cloned into the binary vectors p2YN and p2YC to generate p2YC-DUYAO and p2YN-OsCOX11 recombinant constructs. They were then transformed into *Agrobacterium tumefaciens* strain EHA105 and cultured at 28°C for four days. For transient expression, different combinations of *Agrobacterium tumefaciens* carrying different constructs at an OD_{600} of 0.1 were co-infiltrated with p19 strain into 4∼5 weeks-old *N.benthamiana* leaves as described previously.[61] Three days after transfection, the infiltrated leaves were observed under a confocal laser scanning microscope (Leica SP8). Primers used for amplification are listed in Table S7.

Firefly luciferase complementation imaging (LCI) assay

To detect the interaction between DUYAO and JIEYAO, the coding sequences of *DUYAO* and *JIEYAO* were cloned into pCAMBIA-cLUC and pCAMBIA-nLUC vectors to generate DUYAO-cLUC and JIEYAO-nLUC fused proteins, respectively. Then, the EHA105 strains carrying each of the two constructs, along with negative controls, were co-infiltrated with p19 strain into tobacco leaves. After three days, the infiltrated leaves were incubated with 1 mM luciferin and measured using Tanon 5200 chemiluminescent imaging system. Primers used for amplification are listed in Table S7.

Pull-down assay

For pull-down assay, the full-length coding region of *DUYAO* was cloned into pMAL-c2X vector to generate recombinant MBP-DUYAO protein; and *OsCOX11* was cloned into pMAL-c2X and pCold TF vectors to obtain recombinant MBP-OsCOX11 and His-OsCOX11 proteins, respectively. The constructs were then transformed into *Escherichia coli* DE3 cells, and the strains were cultured at 16°C, 160 r/min for 16 h, and then induced by 0.1 mM isopropyl β-D-1-thiogalactopyranoside to express the fused proteins. MBP-DUYAO and MBP-OsCO11 coupled beads were used to capture His-OsCOX11 to test DUYAO-OsCOX11 and OsCOX11-OsCOX11 interactions, and the effect of MBP-DUYAO on the OsCOX11-OsCOX11 interaction was examined by MBP-DUYAO gradients. The purified protein was first incubated with the corresponding resin (20-30 μL) in 1 mL PBS solution for 1 h with gentle rotation. Then the prey protein fused with a different tag was added. After further 2 h incubation, the resin was washed 5 times with PBS and diluted with 5×protein loading buffer. Finally, the protein samples were carried out for SDS-PAGE and immunoblot analyses with anti-MBP and anti-His antibodies.[62] Primers used for amplification are listed in Table S7.

Co-immunoprecipitation (Co-IP) assay

The full-length coding sequence of *OsCOX11* and *JIEYAO*, each driven by the *Ubiquitin*-1 promoter, was tagged to generate OsCOX11-FLAG and JIEYAO-FLAG fused proteins, respectively. Different combinations of DUYAO-GFP, OsCOX11-FLAG, and JIEYAO-FLAG were transformed into rice protoplasts for transient expression. After 16 h *in vivo* culture, total protein was extracted using native extraction buffer 1(NB1) (50 mM Tris-MES, pH=8.0, 0.5 M Sourose, 1 mM $MgCl_2$, 10 mM EDTA, 5 mM DTT, and 1×Complete Protease Inhibitor Cocktail) and then incubated with Anti-GFP mAb-Magenetic agarose at 4°C for 1 h with shaking. After washing 3 times with NB1 buffer, the protein samples were eluted, and then SDS-PAGE and western blot were performed. Primers used for amplification are listed in Table S7.

Protein purification, pull-down, and gel filtration assays

The full length coding sequence of *DUYAO* was cloned into modified pFastBac vector with a C-terminal Strep tag; the *JIEYAO* coding sequence (1-451 amino acids) was cloned into modified pFastBac vector with a N-terminal 6×His-sumo tag; the *OsCOX11* coding sequence (90-244 amino acids) was cloned into modified pFastBac vector with a N-terminal GST tag. All these proteins were expressed using the Bac-to-Bac baculovirus expression system (Invitrogen) in Sf21 cells at 28°C. Sf21 cells were grown in ESF 921 medium (Expression Systems) by shaking at 120 rpm at 28°C until the cell density reached 2.0×10^6 cells per milliliter. One liter of cells (2.0×10^6 cells per milliliter) was infected with 25 mL of recombinant baculovirus. For protein purification, the cell pellet was harvested via centrifuging the cell mixture after 48 h of infection. The pellet was re-suspended in buffer containing 150 mM NaCl and 25 mM Tris-HCl (pH 8.0). After sonication and centrifugation, the DUYAO-Strep protein was purified by Strep beads; the DUYAO-OsCOX11 complex was purified by Strep beads at first, then the elution of *d*-Desthiobiotin was purified by GST beads again; the DUYAO-JIEYAO complex was purified by Strep beads at first, then the elution of *d*-Desthiobiotin was purified again following the Ni-NTA (Novagen) protocol. All above three elution proteins were further purified by size exclusion chromatography (Superose 6, 10/30, GE Healthcare) in a buffer containing 10 mM Bis-Tris (pH 8.0) and 100 mM NaCl. The peak fraction was separated by SDS-PAGE gel, and proteins were detected by Coomassie blue staining. Primers used for amplification are listed in Table S7.

Expression pattern analysis

About 4 kb-long promoter region of *DUYAO* and *JIEYAO* were amplified and fused to the *RUBY* gene.[33] The constructs were then transformed into T65 calli via *Agrobacterium tumefaciens*-mediated transformation. Whole genomic sequencing was performed to screen for transgenic T_0 plants carrying a single copy of *pDUYAO::RUBY* or *pJIEYAO::RUBY*. Photos were taken when the tissues or organs exhibited red color. Primers used for amplification are listed in Table S7.

"Cytotoxicity-detoxification" test in yeast

To generate *DUYAO*, *DUYAOΔ* and *JIEYAO* under the control of the *alcohol dehydrogenase1* (*Adh1*) promoter used in yeast expression assays, we synthesized all sequences by GenScript (Nanjing, China). For the *pADH1::DUYAO* and *pADH1::DUYAOΔ* constructs, the sequences were amplified by PCR and ligated into the PCR linearized PUG6-NEO-BLANK binary vector. For the *pADH1::JIEYAO* construct, the sequence was amplified by PCR and ligated into the PCR linearized YEB-NAT-BLANK (gift from Professor Fengyan Bai) binary vector. The constructs were then transformed into *Saccharomyces cerevisiae* strain s228c as described above in the Y2H assay section. Primers used for amplification are listed in Table S7.

S2 cell culture and treatment

The coding sequence of *DUYAO* and *JIEYAO* were optimized and synthesized by GenScript, prior to inserting into pUASTattB vector (gift from Dr. Stephen Cohen) to generate *pUAS::DUYAO* and *pUAS::JIEYAO* constructs. Different combinations of *pActin::Gal4* (gift from Dr. Cai Yu), *pUAS*, *pUAS::DUYAO*, and *pUAS::JIEYAO* constructs were then transfected into S2 cells using Effectene Transfection Reagent (Qiagen 301425). Expression of *DUYAO* or *JIEYAO* in *Drosophila melanogaster* S2 cells is driven by an upstream activating sequence (UAS) that is activated upon presence of GAL4. S2 cells were cultured at 25°C in SFM medium (Hyclone) supplemented with 10% FBS (Gibco). After 3, 5, and 7 days of cultivation, the cell absorbance was measured using cell counting kit-8 (CCK-8) (APExBIO). Primers used for amplification are listed in Table S7.

Evolution and haplotype analysis of the *RHS12* locus

Diverse wild and cultivated rice accessions were used to isolate *DUYAO* and *JIEYAO* by PCR and the amplified genomic fragments were sequenced. Sequences alignment for *DUYAO* and *JIEYAO* among accessions was performed by MEGA X software. After that, we input the obtained files into DnaSP6 software, assigned the coding regions, removed the noncoding region, and eventually obtained the haplotypes of *DUYAO* and *JIEYAO*. All the sequenced rice accessions are listed in Table S2.

QUANTIFICATION AND STATISTICAL ANALYSIS

For quantification of pollen fertility and GFP signals, images were analyzed and processed using Adobe Photoshop CS6 software (https://www.adobe.com/cn/products/photoshop.html). All statistical analyses were completed in Graphpad Prism 8 software

(https://www.graphpad.com/scientific-software/prism/). One-way ANOVA and Tukey's test were performed for multiple comparisons test, and detailed descriptions of statistical analyses can be found in the figure legends. All data are presented as mean ± SD.

ADDITIONAL RESOURCES

This study did not generate any additional resources.

Supplemental figures

CellPress
OPEN ACCESS

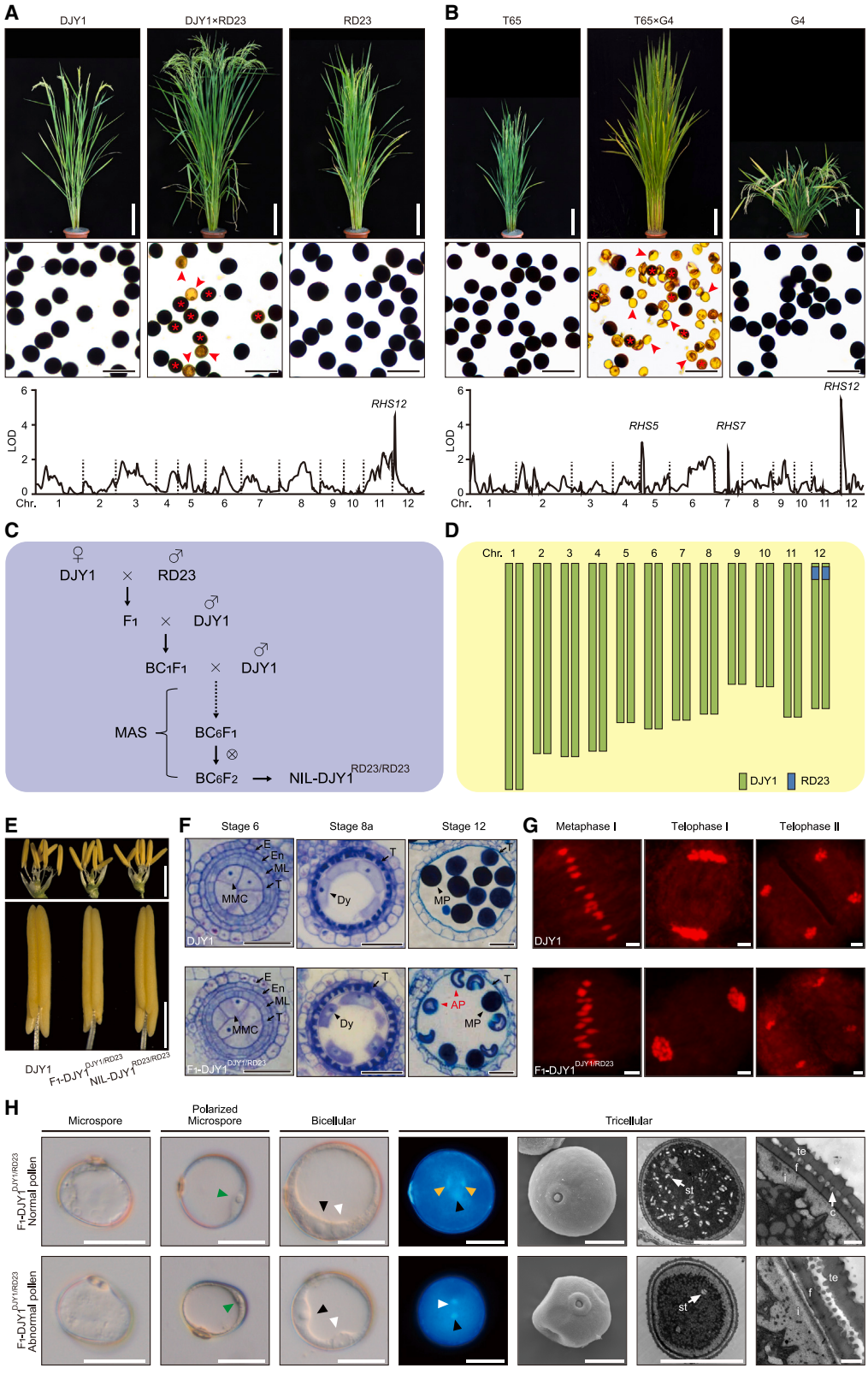

(legend on next page)

Figure S1. Isolation and characterization of *RHS12*, related to Figure 1

(A) Plant morphology (top) and pollen phenotype (middle) of DJY1, RD23, and their hybrid F_1 (DJY1 × RD23), and QTL detection of pollen sterility in the F_2 population (bottom). Arrowheads and asterisks indicate aborted pollen grains and pollen grains with reduced starch accumulation, respectively. Scale bars, 20 cm (top) and 100 μm (middle).

(B) Plant morphology (top) and pollen phenotype (middle) of T65, G4, and their hybrid F_1 (T65 × G4), and QTL detection of pollen sterility in the F_2 population (bottom). Arrowheads and asterisks indicate aborted pollen grains and pollen grains with reduced starch accumulation, respectively. Scale bars, 20 cm (top) and 100 μm (middle).

(C) The strategy for the NIL (NIL-DJY1$^{RD23/RD23}$) construction using RD23 as the donor parent and DJY1 as the recurrent parent. MAS, marker assisted selection.

(D) The graphical genotype of the NIL-DJY1$^{RD23/RD23}$.

(E) Comparison of the flowers (top) and anthers (bottom) between DJY1, NIL-DJY1$^{RD23/RD23}$, and their hybrid F_1 (F_1-DJY1$^{DJY1/RD23}$). Scale bars, 3 mm (top) and 1 mm (bottom).

(F) Transverse sections of anther locules at different developmental stages of DJY1 and F_1-DJY1$^{DJY1/RD23}$. E, epidermis; En, endothecium; ML, middle layer; T, tapetum; MMC, microspore mother cell; Dy, dyad; MP, mature pollen; AP, aborted pollen. Scale bars, 50 μm.

(G) Observation of meiotic chromosome behaviors in DJY1 and F_1-DJY1$^{DJY1/RD23}$. Scale bars, 50 μm.

(H) Observation of F_1-DJY1$^{DJY1/RD23}$ pollen grains at different developmental stages. The first to third (from left) panels show early-stage pollen grains imaged using differential interference contrast (DIC) microscope. Note a pollen arrested at polarized microspore stage. The fourth panel shows pollen grains stained with DAPI (4′, 6-diamidino-2′-phenylindole). The fifth panel is scanning electron micrographs highlighting a caved pollen. The last two pairs of panels are transmission electron micrographs highlighting an abnormal pollen with few starch granules and abnormal wall. St, starch granules; i, intine; f, foot layer; c, columella; te, tectum. Nuclei, vegetative nuclei, generative cells, and sperm cells are indicated by green, black, white, and yellow arrowheads, respectively. Scale bars, 25 μm in the first to sixth panels and 1 μm in the last panels.

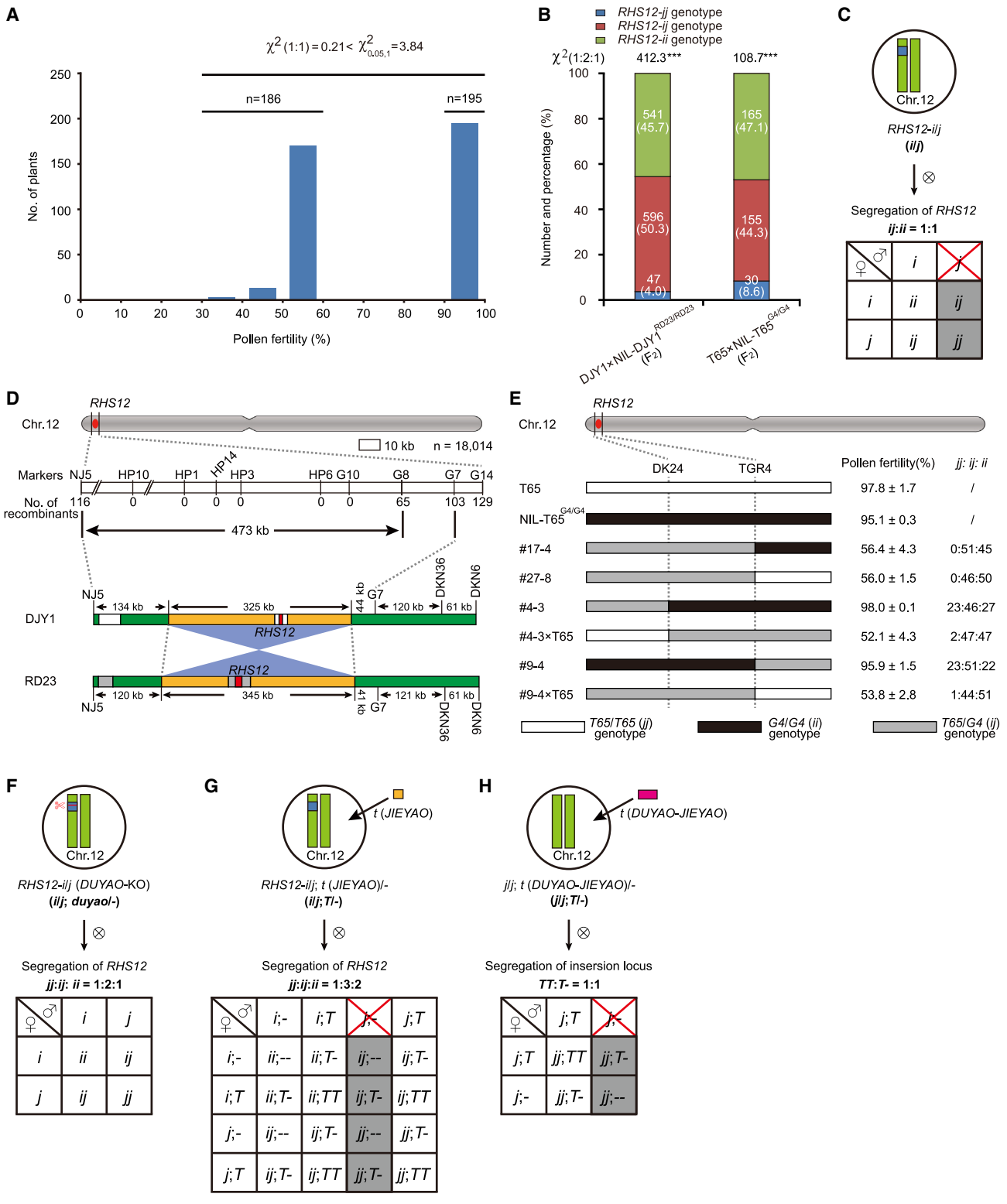

Figure S2. Map-based cloning of *RHS12*, related to Figures 1 and 2

(A) Frequency distribution of pollen fertility in the DJY1 × NIL-DJY1$^{RD23/RD23}$ F_2 population.

(B) Segregation rate of the *RHS12* genotypes in F_2 populations derived from T65 × NIL-T65$^{G4/G4}$ and DJY1 × NIL-DJY1$^{RD23/RD23}$. *ii*, *jj*, and *ij* represent homozygous *indica*, homozygous *japonica*, and heterozygous *indica/japonica* genotype, respectively.

(legend continued on next page)

(C) Diagram of genotypic segregation ratio in the progeny of the *RHS12* heterozygous plant. The segregation of *ii*:*ij* genotype fits a 1:1 ratio due to selective abortion of the *RHS12-j* male gametes (marked by the red "×"). *i* and *j* represent the *indica* and *japonica* allele, respectively.
(D) Mapping of the *RHS12* locus using the DJY1 × NIL-DJY1$^{RD23/RD23}$ F_2 population. The *RHS12* locus was mapped to a genomic region with a chromosome inversion structure (highlighted in yellow) between DJY1 and RD23. The numbers of recombinants are shown under the markers.
(E) Fine mapping of the *RHS12* locus using the T65 × NIL-T65$^{G4/G4}$ F_2 population. Pollen fertility of the recombinant individuals and genotypic segregation at the *RHS12* locus among their progeny are provided.
(F) The genotypic segregation ratio among progeny of *RHS12* heterozygous plants is expected to restore to 1:2:1 when *iORF3*/*DUYAO* is knocked out using the CRISPR-Cas9 technology.
(G) Diagram of the expected segregation ratio of *jj*:*ij*:*ii* genotypes among progeny from *RHS12* heterozygous plants harboring a single copy of the *iORF4*/*JIEYAO* transgene (denoted as *T*).
(H) The expected genotypic segregation ratio among progeny from transgenic heterozygous *japonica* plants harboring a single copy of the *DUYAO*-*JIEYAO* transgene (denoted as *T*).

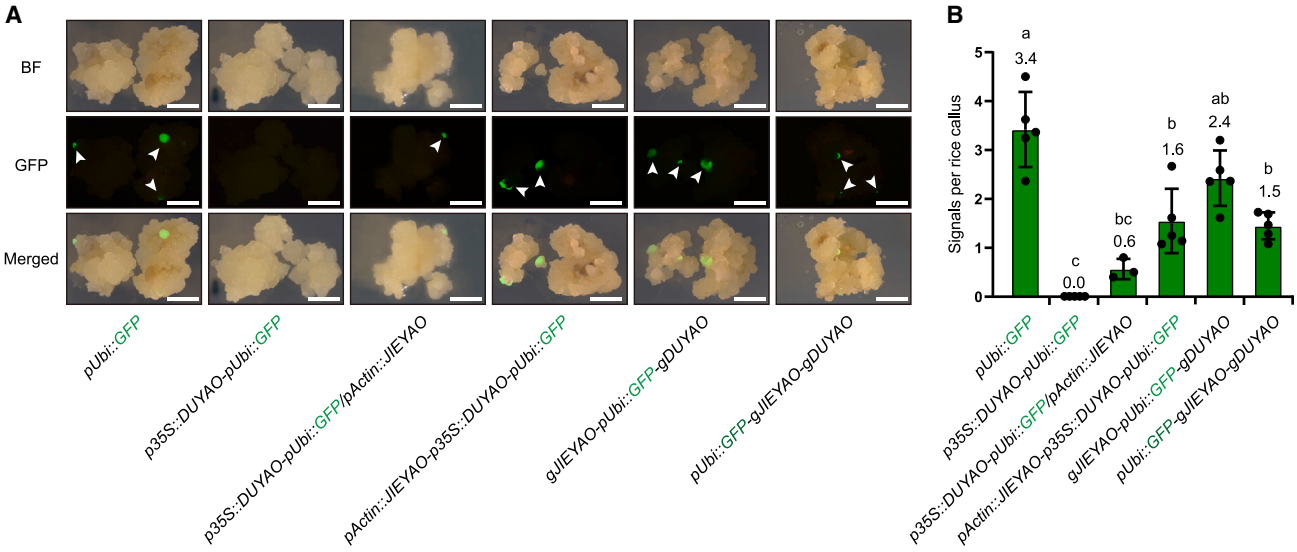

Figure S3. Cytotoxicity-detoxification analysis of the *DUYAO-JIEYAO* element, related to Figure 2

(A) Monitoring of cytotoxicity-detoxification using the *GFP* reporter in T65 calli cells. Various combinations of *DUYAO* and *JIEYAO* constructs were co-transformed with the *pUbi::GFP* reporter into T65 calli. GFP signals (indicated by the arrowheads) were observed under fluorescence microscope for 2 weeks after being cultured on selection medium. Scale bars, 2 mm.

(B) Quantification of GFP signals per callus shown in (A). Data are presented as mean ± SD, n = 5, 5, 3, 5, 5, and 5 plates (10 calli per plate) for the six treatments in (A), respectively. Different letters were obtained by ANOVA and Tukey's test, indicating significant differences ($p < 0.01$).

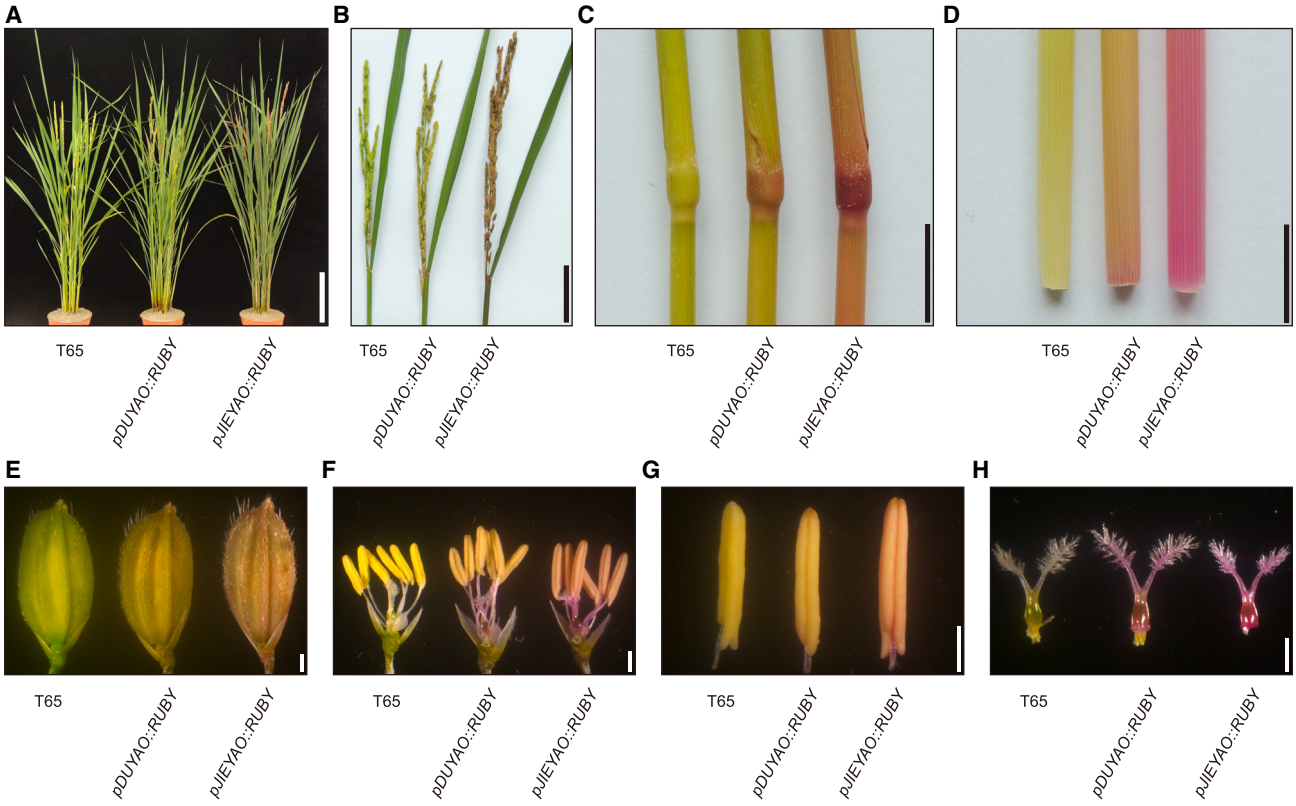

Figure S4. Expression pattern of *DUYAO* and *JIEYAO*, related to Figure 3

The promotor of *DUYAO* or *JIEYAO* was cloned and used to drive the *RUBY* reporter gene. Transgenic plants carrying single-copy *pDUYAO::RUBY* (middle) or *pJIEYAO::RUBY* (right) were observed for red color in whole plants (A), panicles and leaves (B), stem nodes (C), stems (D), spikelets (E), flowers (F), anthers (G), and pistils (H). Wild-type T65 (left) as the control is dominated by green color. Scale bars: 20 cm in (A); 5 cm in (B); 1 cm in (C) and (D); and 1 mm in (E)–(H).

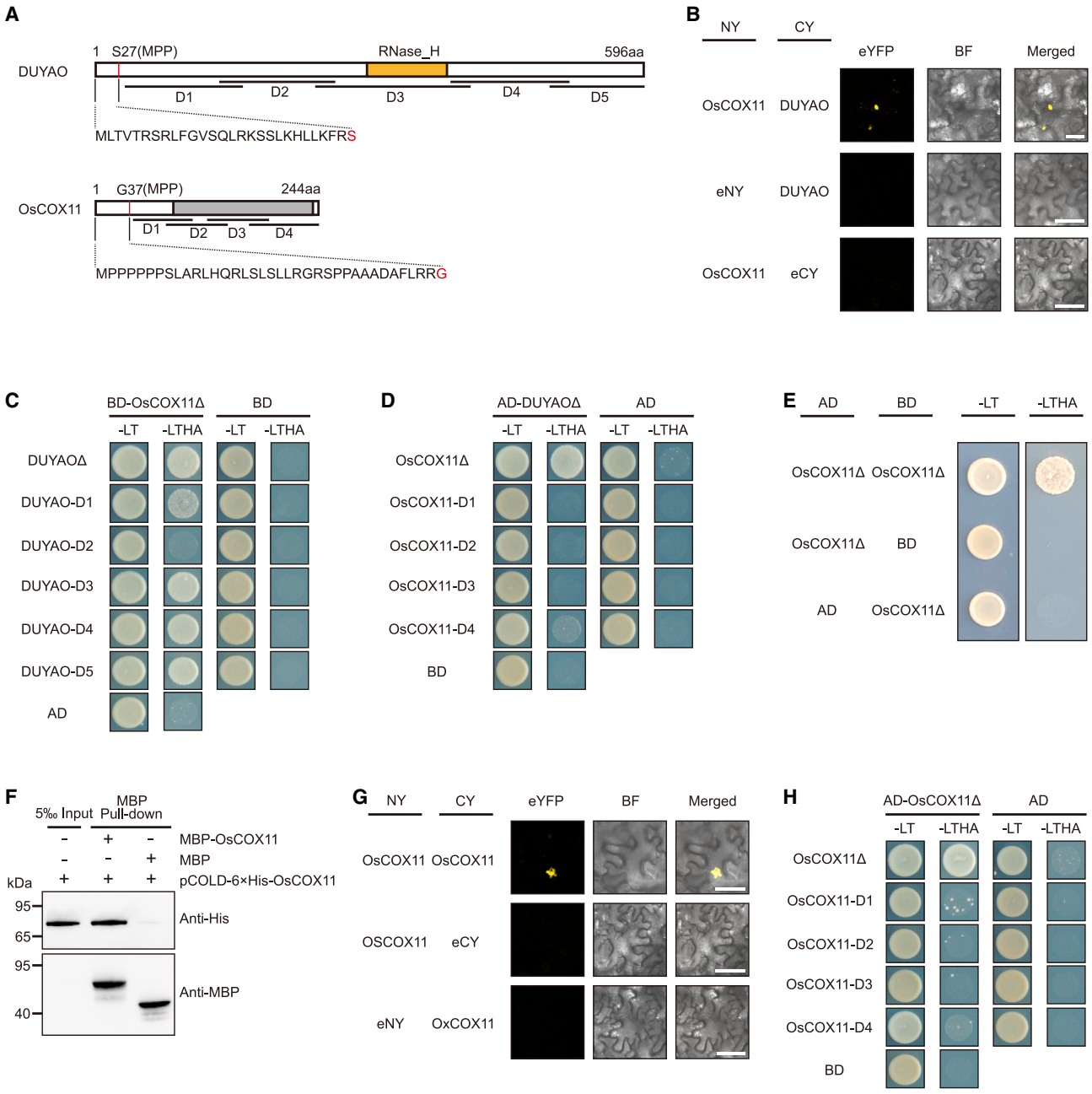

Figure S5. Interaction between DUYAO and OsCOX11, and self-interaction of OsCOX11, related to Figure 3

(A) Schematic structure of DUYAO and OsCOX11 and their truncations for Y2H assay. Red lines indicate the cleaved-off position by the heterodimer mitochondrial processing peptidase (MPP). The amino acid sequence of the predicted mitochondrial signal peptides are provided (http://mitf.cbrc.jp/MitoFates/cgi-bin/top.cgi). Yellow and gray boxes represent the ribonuclease H (RNase_H) domain (http://www.ebi.ac.uk/interpro/) and CtaG_Cox11 domain (http://smart.embl-heidelberg.de/), respectively.

(B) BiFC assay of OsCOX11 and DUYAO in *N. benthamiana*. eYFP, enhanced yellow fluorescent protein. NY, N-terminals of YFP; CY, C-terminal of YFP; BF, bright-field image. Scale bars, 50 μm.

(C) Y2H assay showing interaction of OsCOX11Δ with different truncated versions of DUYAO. DUYAOΔ and OsCOX11Δ indicate their truncated version without the mitochondrial signal. The various truncated versions of DUYAO are shown in (A).

(D) Y2H assay showing interaction of DUYAOΔ with different truncated versions of OsCOX11. The various truncated versions of OsCOX11 are shown in (A).

(E) Y2H assay showing that OsCOX11Δ could interact with itself.

(F) OsCOX11 interacts with itself in a pull-down assay.

(G) BiFC assay showing self-interaction of OsCOX11. Scale bars, 50 μm.

(H) Y2H assay showing interaction of OsCOX11Δ with different truncated versions of OsCOX11.

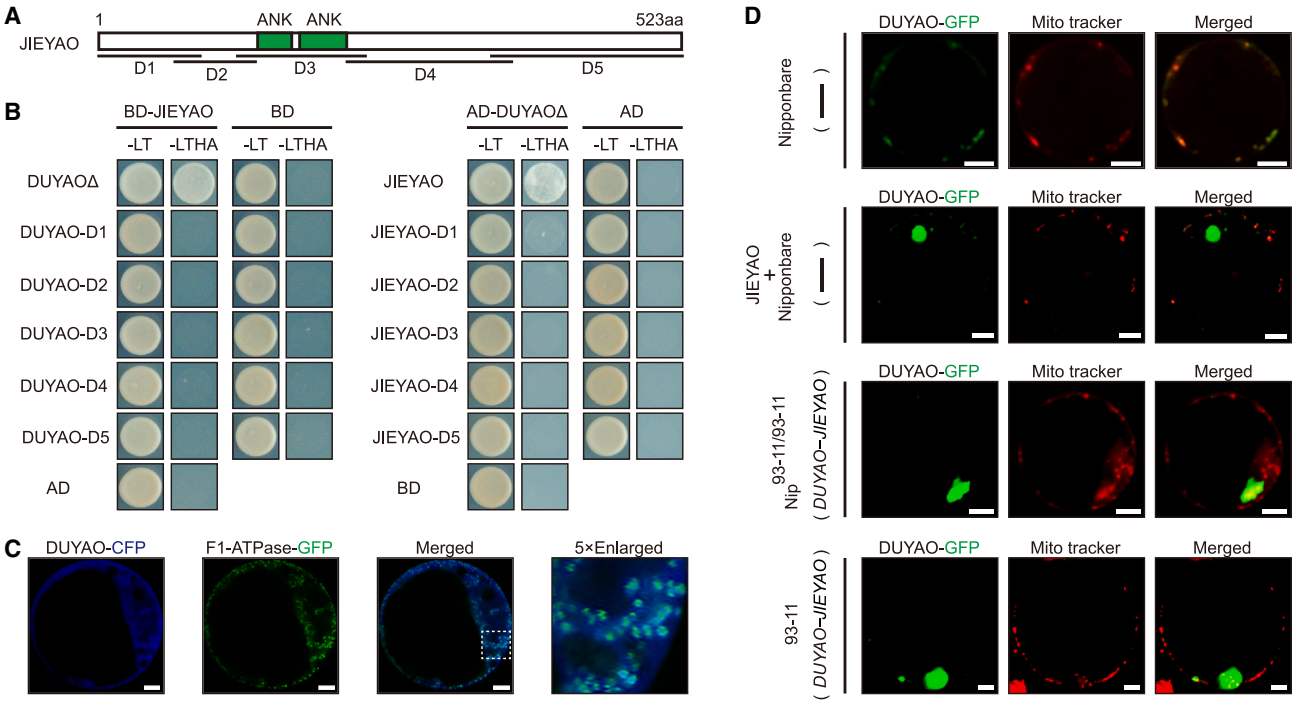

Figure S6. Interaction between DUYAO and JIEYAO and subcellular localization of DUYAO in presence of JIEYAO, related to Figure 4

(A) Schematic structure of JIEYAO. Green boxes represent the ankyrin (ANK) repeats domain (http://smart.embl-heidelberg.de/). Fragmented versions of JIEYAO for Y2H are shown.

(B) JIEYAO interacts with DUYAOΔ (truncated version with the mitochondrial signal removed), whereas truncation of either DUYAO or JIEYAO abolishes the interaction. Refer to Figure S5 for truncations of DUYAO.

(C) Subcellular localization of DUYAO-CFP and F1-ATPase-GFP (marker for mitochondria) in protoplasts isolated from *Arabidopsis* suspension cells. Scale bars, 5 μm.

(D) DUYAO is not localized to mitochondria in the presence of JIEYAO. *DUYAO-GFP* was expressed alone or co-expressed with *JIEYAO* in leaf sheath protoplasts of Nipponbare (*japonica* background without endogenous *DUYAO-JIEYAO*). In an alternative approach, *DUYAO-GFP* was expressed in protoplasts derived from 93-11 (*indica* background with intrinsic *DUYAO-JIEYAO*) or from NIL-Nip$^{93\text{-}11/93\text{-}11}$ (a near-isogenic line in the Nipponbare background with the *DUYAO-JIEYAO* element introgressed from 93-11). Note that DUYAO-GFP is no longer lined up with the mitochondrial tracker in the presence of JIEYAO. Scale bars, 5 μm.

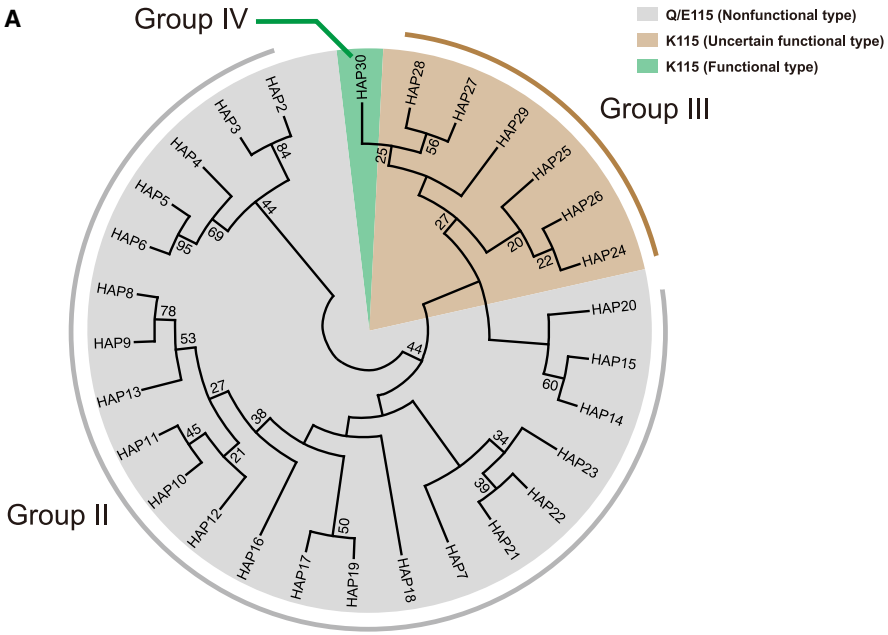

B

Fully fertile Semi-sterile

Donor species (variety)	Genotype	*O. rufipogon-1*	*indica* (RD23)	*O. rufipogon-2*	*indica* (Dular)	*O. rufipogon-3*	*Japonica* (DJY1)
O. rufipogon-1 (acc.81986)	*DUYAO-JIEYAO*	●					
indica (RD23)	*DUYAO-JIEYAO*	●	●				
O. rufipogon-2 (acc.80581)	$duyao^{T/S}$-$jieyao^{S}$	●	●	●			
indica (Dular)	$duyao^{T/S}$-$jieyao^{S}$	●	●	●	●		
O. rufipogon-3 (acc.103308)	—	●	●	●	●	●	
Japonica (DJY1)	—	●	●	●	●	●	●

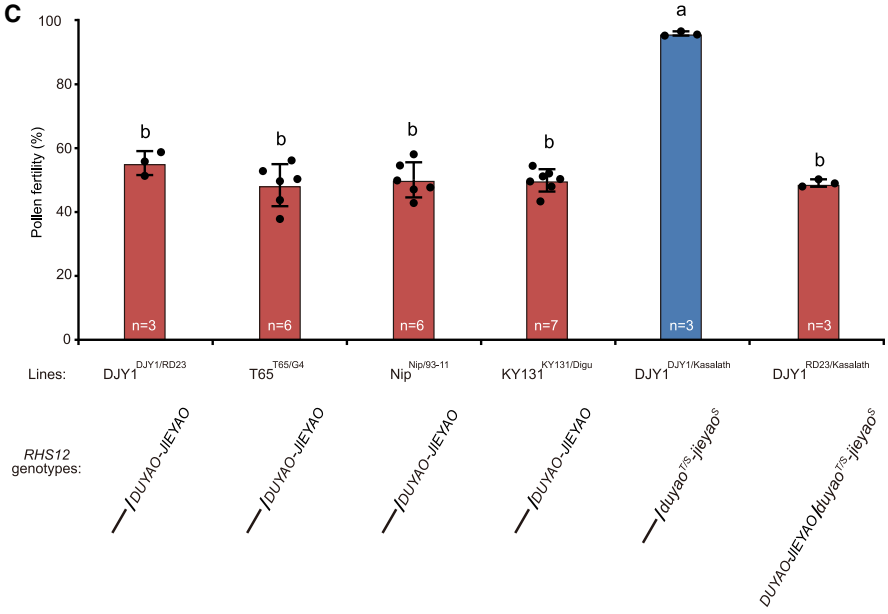

(legend on next page)

Figure S7. Relationship analysis of 30 JIEYAO haplotypes and hybrid pollen fertility test using crosses between NILs carrying the *RHS12* locus of different origins, related to Figure 5

(A) Neighbor-joining tree of JIEYAO showing the relationship of 30 haplotypes (forming three distinct groups shown in different colors). The tree was constructed in MEGA X. Hap-1 is not shown as it lacks the corresponding sequences.

(B) F_1 pollen fertility of cross combinations between different NILs in a diallel set. All the NILs are in DJY1 background but with the *RHS12* locus separately introgressed from three wild rice species (*O. rufipogon*) and two Asian cultivated rice (Dular and RD23). *RHS12* genotype is denoted as functional *DUYAO-JIEYAO*, nonfunctional $duyao^{T/S}$-$jieyao^{S}$ or absence (–).

(C) F_1 pollen fertility of crosses between NILs of different genetic backgrounds. All F_1 plants are heterozygous at the *RHS12* locus regardless of its functionality. Digu and Kasalath are *indica* varieties, carrying functional *DUYAO-JIEYAO* element and nonfunctional $duyao^{T/S}$-$jieyao^{S}$ element, respectively. Data are presented as mean ± SD. Different letters indicate significant differences ($p < 0.001$) by ANOVA and Tukey's test.